DISCLAIMER

This report was prepared as an account of work sponsored by an agency of the United States Government. Neither the United States Government nor any agency thereof, nor any of their employees, makes any warranty, express or implied, or assumes any legal liability or responsibility for the accuracy, completeness, or usefulness of any information, apparatus, product, or process disclosed, or represents that its use would not infringe privately owned rights. Reference herein to any specific commercial product, process, or service by trade name, trademark, manufacturer, or otherwise does not necessarily constitute or imply its endorsement, recommendation, or favoring by the United States Government or any agency thereof. The views and opinions of authors expressed herein do not necessarily state or reflect those of the United States Government or any agency thereof. Reference herein to any social initiative (including but not limited to Diversity, Equity, and Inclusion (DEI); Community Benefits Plans (CBP); Justice 40; etc.) is made by the Author independent of any current requirement by the United States Government and does not constitute or imply endorsement, recommendation, or support by the United States Government or any agency thereof.

DIRECT PROCESSING OF LITHIUM CHLORIDE BASED WASTE SALT IN A CERAMIC WASTE FORM

Nuclear Fuel Cycle & Supply Chain

Prepared for
U.S. Department of Energy
Materials Recovery and Waste Form Development Campaign

J.E. Gesualdi, E. Schneiderlochner, Y. Liao, J. Rojas, and W.L. Ebert
Argonne National Laboratory

February 27, 2026
ANL/CFCT-26/3

ABSTRACT

Ceramic waste form materials were fabricated with a LiCl based salt mixture to demonstrate the suitability of direct processing of waste salt from an all LiCl pyroprocessing flow sheet on the formation, microstructure, and durability of ceramic waste forms. Materials were successfully synthesized by using the simplified direct processing technique with salt loadings of 5, 7.5, and 10 wt% at the laboratory scale. Materials fabricated with LiCl based salt indicated full conversion of zeolite to sodalite occurred to form products with low open porosity. This indicates that the Na_2O content of NBS4 glass is suitable for processing salt chemistries which do not contain NaCl. Generated sodalite was microencapsulated by the glass binder, halite occlusions were detected within sodalite domains at all salt loadings, and a Cs-rich phase believed to be Cs-pollucite was detected in the material made with the lowest salt loading (5 wt%). Salt inclusions were encapsulated within the binder glass at all loadings, and found to consist primarily of NaCl with Cs present. A small amount of salt was found at the surface of the wasteform made with the highest salt loading of 10 wt%, which may indicate an upper limit to the amount of salt that can be accommodated or incomplete mechanical mixing of the reagents.

Durability testing by using the ASTM C1308 method indicated that initial rapid dissolution of exposed halite inclusion phases was directly correlated to salt loading. Wasteform degradation during all tests occurred primarily due to dissolution of the sodalite phase. Durability of the binder glass was found to increase as the waste salt loading increased. Results for the release of cations from the salt indicate the changes in wasteform durability and halite inclusion chemistry are strongly influenced by ion exchange phenomena between the salt and the glass. This appears to be the result of the relatively stronger affinity for the glass phase of Li, compared to that of other cations such as Na and Cs. The effects from cation exchange were diminished at lower salt loadings.

THIS PAGE INTENTIONALLY LEFT BLANK

CONTENTS

FIGURES

TABLES

ACRONYMS AND ABBREVIATIONS

ACWF	Advanced sodalite Ceramic Waste Form
ANL	Argonne National Laboratory
ASTM	ASTM-International
BSE	Backscattered Electron (image)
BSG	Borosilicate Glass
CWF	Ceramic Waste Form
DOE	US Department of Energy
EDS	Energy-Dispersive X-ray Emission Spectroscopy
HIP	Hot Isostatic Pressing
INL	Idaho National Laboratory
MRWFD	Material Recovery & Waste Form Development (campaign)
NBS	Sodium Borosilicate (glass)
PC	Pressureless Consolidation
PNNL	Pacific Northwest National Laboratory
RH	Relative Humidity
SCWF	Simplified Ceramic Waste Form
SEI	Secondary Electron Image
SEM	Scanning Electron Microscope (or microscopy)
XRD	X-ray Diffraction

THIS PAGE INTENTIONALLY LEFT BLANK

ACKNOWLEDGEMENTS

This report was produced under the auspices of the US DOE Office of Nuclear Energy Nuclear Fuel Cycle & Supply Chain program Materials Recovery and Waste Form Development Campaign. Issuance of this report meets milestone M3FT-25AN0301040112 and M3FT-26AN0301040116. Zeolite 4A materials were provided by Dr. Morgan Kropp and colleagues at the Idaho National Laboratory (INL) and NBS4 glass was provided by Dr. Brian Riley and colleagues at Pacific Northwest National Laboratory (PNNL). Solution analyses provided by Ms Yifen Tsai (Argonne Analytical Chemistry Laboratory) are gratefully acknowledged.

This work was conducted at Argonne National Laboratory and supported by the U.S. Department of Energy, Office of Nuclear Energy, under Contract DE-AC02-06CH11357.

THIS PAGE INTENTIONALLY LEFT BLANK

MATERIALS RECOVERY & WASTE FORM DEVELOPMENT CAMPAIGN

Direct Processing of Lithium Chloride Based Waste Salt in a Ceramic Waste Form

1. INTRODUCTION AND BACKGROUND

The glass-bonded sodalite ceramic waste form (CWF) was designed in the 1990's to accommodate chloride ions in salt waste within the crystal structure of synthetic sodalite ($Na_8[Al_6Si_6O_{24}]Cl_2$) that is then microencapsulated in a durable borosilicate glass matrix (see Ebert 2005 and references therein). The conversion of Zeolite 4A to sodalite occurs by reaction of NaCl in the salt with the reaction stoichiometry given in Equation 1.

$$\underset{\text{zeolite 4A}}{Na_{12}(AlSiO_4)_{12}} + 4NaCl \rightarrow 2\ \underset{\text{sodalite}}{Na_8(AlSiO_4)_6Cl_2} \quad (1)$$

The process developed to produce large-size CWF products that would fit in a standard DOE disposal canister from pyroprocessing salt waste is depicted in Figure 1. Process steps include crushing, milling, and sizing solid waste salt, crushing, milling, and sizing binder glass, and crushing, milling, sizing, and drying commercial Zeolite 4A. The sized salt and Zeolite 4A were mixed first at 500 °C to occlude the salt within the cage structure of the zeolite with only a small amount of salt on the particle surfaces. The amount of so-called "free chloride" was measured to confirm the added salt was almost completely contained within the zeolite particles prior to processing. The salt-containing zeolite was then blended with sized glass frit and heated to at least 850 °C to process. Initially, the mixture was placed in a collapsable steel canister and processed by using hot isostatic pressing (HIP). It was later determined that pressurization was not necessary for effective stabilization. A pressureless consolidation method (referred to herein as the baseline PC method) was demonstrated to be suitable for processing mixtures of salt-containing zeolite and glass in a full-size DOE disposal canister and has been used since 2000 (Priebe and Bateman 2007).

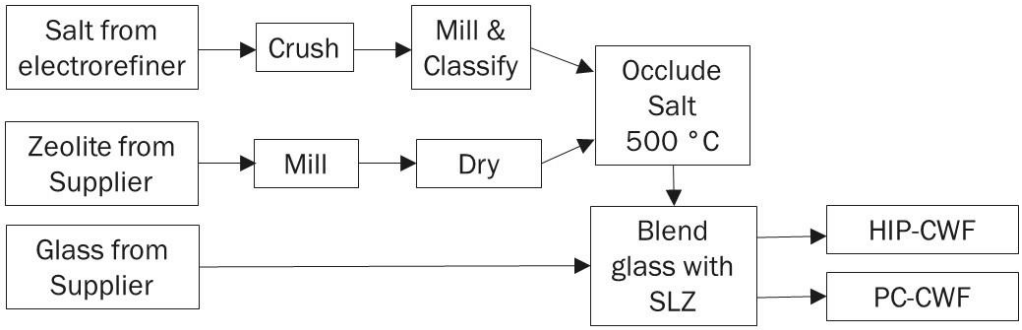

Figure 1. Flow diagram showing steps in baseline PC method for producing CWF.

Developmental research in the early 2000's demonstrated that (1) salt that had been occluded in the zeolite prior to processing migrated out of the zeolite framework and into the glass during processing, and (2) that some salt constituents (preferentially actinide and lanthanide elements) were oxidized by residual water in the zeolite during the occlusion process and decorated the surfaces of the aggregated particles (Ebert 2005). This suggested that, while the salt occlusion step provided control of the salt:zeolite stoichiometry, it was not necessary for the conversion reaction given in Eq. 1 to occur effectively. Further research demonstrated that the binder glass can be utilized to provide additional sodium to generate more sodalite to accommodate more chlorine and increase salt loading significantly (Ebert et al. 2017). It has been hypothesized that the production of CWF can be accomplished by simplifying the process depicted in Figure 1 without significantly decreasing the salt waste loading or waste form durability. Specifically, it has been hypothesized that the reagent size and dryness controls can be relaxed significantly to facilitate handling in a hot cell environment, that premixing to occlude salt in the Zeolite 4A pore structure is not necessary, and that the processing temperature can be decreased to 900 °C or lower (Ebert 2024).

Work in the prior fiscal year demonstrated the viability of the simplified ceramic wasteform processing approach (Gesualdi, 2025). Notably, processing at 925 °C for 2 h with materials crushed to -16 +60 size fractions and mechanically mixed successfully produced uniform ceramic wasteform products. Sodalite was successfully generated in situ and encapsulated in binder glass, suggesting that pre-occlusion of salt into zeolite is not a process requirement. The zeolite moisture content, either fully dried or saturated at 48% relative humidity, did not impede sodalite formation. The open porosity observed in wasteform products made with 20 wt% glass was similar to that in CWF made using the baseline method, and was reduced significantly by increasing the glass content to 40 wt%. Porosity of wasteforms made at 880 °C was slightly higher, but complete conversion to sodalite occurred. Halite by-products formed as spherical inclusions encapsulated in the binder glass phase and were not observed to accumulate at the surface of the wasteform due to density based separation. Using larger sized reagent particles (4-8 mesh or 2-6 mm zeolite beads, +14 mesh salt and glass) formed consolidated wasteforms, but the reaction to generate to sodalite was incomplete within the 2-h process duration, with exterior shells of generated sodalite observed surrounding unreacted cores of zeolite. This suggests there would be kinetic limitations to the use of large zeolite particles, but that fairly coarse (>500 μm) materials could be used if given adequate time to react. Follow-on measurements are required to measure the conversion reaction kinetics independent of the heating rate.

With this baseline understanding of the effectiveness of the simplified process, the effect of waste salt chemistry based on modifications to the pyroprocessing flowsheet that are being considered was studied. Work described in this report addresses processing CWF with salt chemistry reflecting waste streams from pyroprocessing operations in a LiCl based electrolyte (rather than LiCl-KCl eutectic) and with elevated active metal fission products (Cs, Sr) to reflect recent improvements in melt crystallization processing of waste salt. The influence of waste salt chemistry from oxide reduction and electrorefining operations is being explored, including waste salts that contain little to no Na content. As NaCl is necessary for sodalite formation, this series of wasteforms will depend entirely on Na provided by a high-soda glass such as NBS4 (~21 wt% Na_2O) to form sodalite. To that end, this work included the effect of various salt loadings (5, 7.5, 10 wt%) to understand the limitations of the available Na_2O in NBS4 glass, as well as the capacity of the glass matrix to capture halite by products within inclusions. In addition, the effect of the higher Li content and possible formation of Li- or Cs-pollucite phases on the glass phase durability is being compared to that of binder glass in CWF materials made with LiCl-KCl waste salt.

2. EXPERIMENTAL APPROACH

The effect of a modified LiCl-based salt chemistry with elevated active metal fission product concentrations on the formation and performance of simplified ceramic wasteforms was assessed by synthesizing small-scale products and evaluating the microstructure and dissolution resistance (chemical durability). These materials were compared to materials having similar compositions that were made using LiCl-KCl based salt in the previous fiscal year. Several materials were made using the simplified direct process to further evaluate the effect of modified salt loadings by shifting the ratio of zeolite:salt from the 7:1 in the stoichiometric reaction. That is, salt content of the wasteform was modified by exchanging directly for zeolite content. All SCWF materials were produced in a muffle furnace within an argon atmosphere glovebox near ambient pressure. Materials were made with a LiCl-based salt to reflect waste salt derived from LiCl-based electrochemical processing of used oxide and metallic used nuclear fuel. All SCWF materials were made using Zeolite-4A that was provided by colleagues at the Idaho National Laboratory, NBS4[1] glass provided by colleagues at Pacific Northwest National Laboratory, and salt synthesized at Argonne.

2.1 Reagent Materials

Salt

The salt mixture referred to as "ORX" was formulated based on the waste salt composition expected after treatment of waste salt removed from the electrorefiner to recover remaining actinides and lanthanides (by electrolytic drawdown) and to recover and recycle a significant portion of the LiCl electrolyte by salt crystallization. This chemistry considers oxide reduction and electrorefining of spent nuclear fuel which is not Na-bonded, and thus introduces no significant Na into the salt. Additionally, higher active metal fission product concentrations are included to reflect improvements in melt crystallization technology. As listed in Table 1, both the ORX and ERX surrogate waste salts are dominated by active metal fission products. Although waste salt to be immobilized is expected to have very low rare earth element concentrations if a lanthanide drawdown operation is used, a small amount of $NdCl_3$ was included in the ORX formulation to support comparisons with the elemental distributions observed in CWF made previously with LiCl-KCl salts similar to ERX by using PC and HIP methods.

Table 1. Composition of ORX and ERX salt, formula wt %

Salt	LiCl	NaCl	KCl	CsCl	$SrCl_2$	$NdCl_3$
ORX	74	-	-	15	9	2
ERX	34	13	43	5	3	2

The ORX salt was synthesized and prepared in an argon atmosphere glovebox maintained with < 0.1 ppm oxygen and < 1 ppm moisture contents. Reagent salts were dried in alumina crucibles at 200 °C for 6 h prior to weighing for the final composition. Appropriate masses (precision within 0.01 g) of dried pure reagent salts (99.5% pure or higher) were mechanically mixed in an alumina crucible and heated to approximately 700 °C for three hours in a furnace housed in an argon atmosphere glovebox maintained with < 0.1 ppm oxygen and < 1 ppm moisture.

[1] Note: NBS4 is an internal designation for a particular glass composition.

The salt was crushed and sieved to isolate the +16, -16 +60 (1.2 – 0.25 mm), and -60 mesh size fractions. (Note: -16 means the particles passed through a 16 mesh sieve and +60 means the particles did not pass through a 60 mesh sieve.) Samples of the bulk salt and crushed pieces were mounted in epoxy and prepared for SEM-EDS analysis to confirm homogeneity. All SCWF materials were made using reagents sized -16 +60 mesh. The salt size for the baseline process is -30 mesh (<0.60 mm) for salt to be occluded in the Zeolite 4A particles prior to processing CWF with the HIP or PC method. The salt occlusion step is omitted in the conceptual simplified process being assessed in which molten salt would instead be added directly to a heated mixture of Zeolite 4A and glass particles. Following the previous work in SCWF production, mechanical mixing was found to have adequately distributed salt throughout the wasteform during processing (Gesualdi et al. 2025).

Binder Glass

The borosilicate glass NBS4 that was formulated to provide additional sodium for generating sodalite in advanced CWF (ACWF) materials made using the PC method was used to make the SCWF materials (Ebert et al. 2017). The composition of NBS4 is given in Table 2. About 200 g of NBS4 glass was provided by colleagues at PNNL. The NBS4 glass was crushed and sieved using a benchtop mill (IKA model A10) and vibratory sieve shaker (ATM Sonic Sifter) to isolate the -16 +30 (1.2 – 0.6 mm), +16, and -30 mesh size fractions. These size fractions are larger than the binder glass size called for in the baseline PC process, which is -60 +325 mesh (0.25 – 0.05 mm). Most SCWF materials described herein were made using the -16 +30 mesh size fraction.

Table 2. Elemental composition of NBS4 glass, oxide mass percent.

SiO_2	61.96%	Al_2O_3	4.20%	B_2O_3	6.30%
Na_2O	21.24%	CaO	4.20%	ZrO_2	2.10%

Zeolite 4A

Commercial Zeolite 4A beads are aggregates of ~5 μm crystallites that are held together with a proprietary clay binder. The mass of the binder is not distinguished from the mass of the Zeolite 4A crystallites in either formulations of SCWF materials or batching reagents. Some beads were crushed and sieved at INL to isolate the -4 +16 (4.75 - 1.20 mm) and -16 +30 (1.20 – 0.60 mm) mesh size fractions. These are both larger than the zeolite size of -60 +325 mesh (0.25 – 0.05 mm) called for in the baseline PC method. Both uncrushed beads and the -16 +30 mesh size fraction were provided by INL for the materials made at Argonne that are discussed herein.

The crushed zeolite materials were preconditioned by equilibration at 48% relative humidity (RH) in a desiccator using a saturated solution of K_2CO_3 to fix the humidity at room temperature (approximately 23 °C). This ensures initial uniformity of residual water contents of Zeolite 4A used to make all SCWF materials at Argonne and INL. Samples of the humidity-equilibrated zeolite were preheated to 300 °C for 2 h to remain consistent with previously made SCWF materials. The prior SCWF work determined that the moisture content of the zeolite did not significantly impede the consolidation of the wasteform or the formation of sodalite at the laboratory scale. However, elevated moisture content within a scaled up process may present technical issues unrelated to wasteform quality, such as the corrosion of equipment due to the combination of moisture, halides, and elevated temperatures.

2.2 Reagent Material Characterization

Most materials were characterized by preparing polished cross sections and analyzing the surfaces using scanning electron microscopy. A Hitachi S-3400N scanning electron microscope (SEM) with an associated backscattered electron (BSE) detector and energy-dispersive X-ray emission spectrometer (EDS; Bruker) was used. Initial characterization included SEM/EDS to determine elemental composition and distribution. Secondary electron imaging (SEI) was used to highlight surface morphologies and BSE imaging was used to highlight and visually distinguish constituent phases having different compositions. Elements with higher atomic numbers scatter more efficiently than elements with lower atomic numbers and appear brighter in BSE images. Most SEM photomicrographs included in this report are of BSE images. Elemental phase compositions were measured by using both spot and small field of view analysis modes and the distributions of individual elements between different phases were visualized using EDS X-ray emission mapping.

Salt

A section of bulk ORX salt and crushed pieces were fixed in epoxy and prepared for SEM analysis. The cross section was prepared by mounting pieces of salt in epoxy and using dry polishing techniques to avoid dissolution in polishing fluid. The microstructure of the ORX salt is shown in the BSE images in Figures 2a and 2b. The bulk salt ingot and salt piece show a dendrite-interdentrite morphology that is a typical solidification microstructure. A higher magnification image and SEM-EDS mapping of the material in the boxed red region in Figure 2a, was performed and is shown in Figure 3. This analysis shows that the dendrites consist of a core of LiCl salt without Cs, Sr, or Nd surrounded by a shell of salt with Cs, which is labeled (Li,Cs)Cl. The interdendritic phase labeled (Cs,Sr)Cl has a vermicular eutectic microstructure and contains the highest concentrations of Cs, Sr, and Nd. This suggests that as the salt solidified, pro-eutectic LiCl crystals precipitated first. As the salt continued to cool, CsCl began to solidify out within the LiCl. The remaining eutectic liquid containing Cs, Sr, and Nd later solidified between the dendrites.

Results of EDS point analyses in the labeled regions of Figure 3a are shown in Table 3 and indicate the dendrite cores consist of >98 at% Cl with very little Cs, Sr, or Nd. As EDS does not detect Li, this phase is likely nearly pure LiCl. The outer shell of the dendrite phase contains approximately 3 at% Cs. However, it is clear even at this length scale that the microstructure in this region is not a solid solution, suggested by variations in brightness, and thus likely has a higher Cs content on average. The interdendritic eutectic phase (Cs,Sr)Cl contains up to 11 and 16 at% Cs and Sr chloride, as well as up to 24 at% oxides suggesting these regions contain the majority of active metal fission products and also oxide-impurities in the salt. Within the eutectic phase is a chemically distinct (Cs,Nd)Cl phase with up to 8 at% Nd. These analyses indicate that the material contains significant chemical inhomogeneity on the micrometer scale. However, this microstructure appears uniform throughout the salt ingot and crushed pieces, suggesting that even small amounts of the crushed and randomly mixed salt would generate a sufficiently chemically homogeneous product.

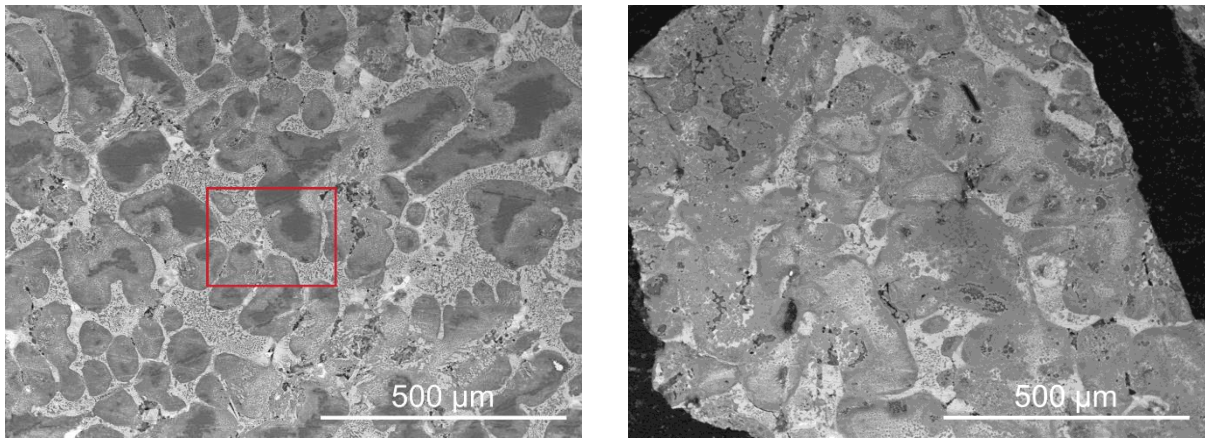

(a) (b)

Figure 2. Photomicrographs of cross-sectioned salt (a) from the bulk cast salt ingot and (b) from crushed grains of salt.

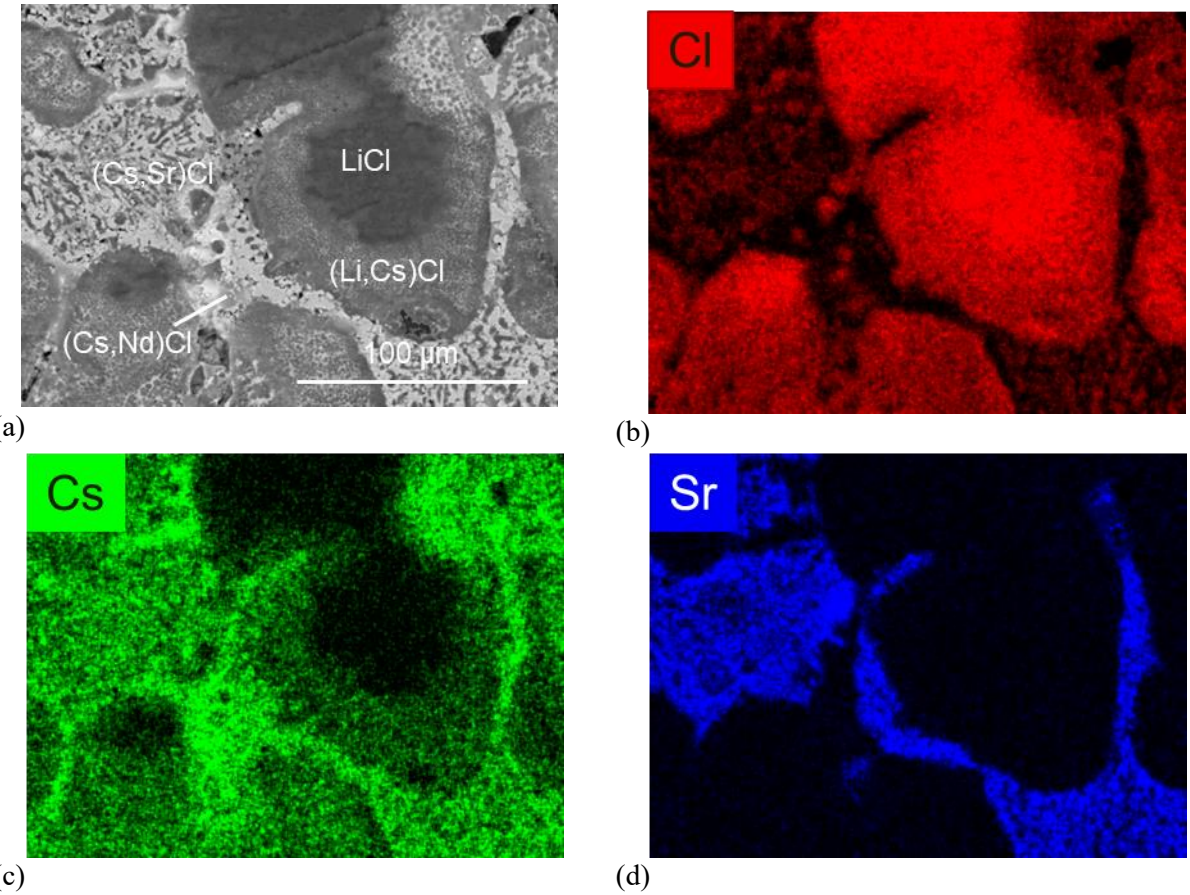

(a) (b)

(c) (d)

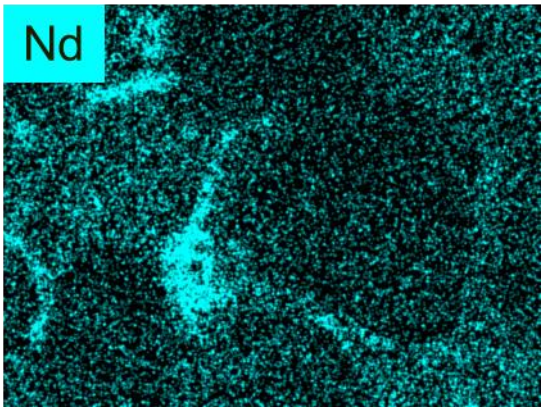

(e)

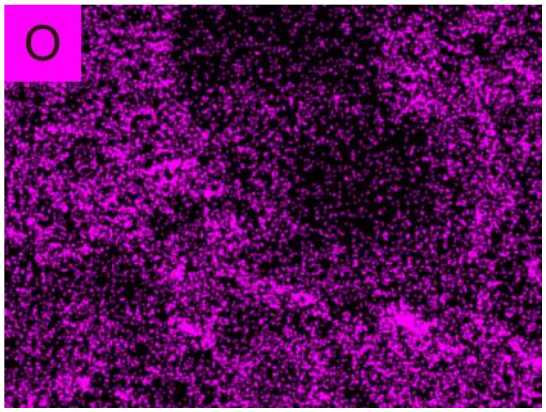

(f)

Figure 3. EDS X-ray elemental maps of region in salt grain: (a) photomicrograph of region and maps of (b) chlorine, (c) cesium, (d) strontium, (e) neodymium, and (f) oxygen.

Table 3. EDS X-ray point analysis results for the regions indicated in Figure 3a, in at %. Note: EDS analysis is not sensitive to Li.

Region	O	Cl	Sr	Cs	Nd
LiCl	1.15	98.46	0.03	0.17	0.00
(Li,Cs)Cl	3.03	93.28	0.33	3.01	0.00
(Cs,Sr)Cl	23.69	48.76	15.81	11.22	0.53
(Cs,Nd)Cl	8.28	62.83	0.76	20.06	7.95

2.3 Material Synthesis and Characterization

Materials were synthesized by mechanically mixing reagents in an alumina crucible and heating in a muffle furnace housed in an argon atmosphere glovebox maintained with less than 30 ppm oxygen. The furnace heating rate was 10 °C/min, and the ramp time was approximately 90 minutes. Table 4 indicates the SCWF compositions that were fabricated. Times indicated in the Thermal Cycle column represent time spent at the process temperature, and does not include the time spent heating or cooling. SCWF-4 was fabricated previously (Gesualdi, 2025) and is included in this table as it was used for direct comparison of LiCl ORX products to those made with the LiCl-KCl ERX salt. Note that a higher glass content is required to encapsulate the larger sodalite domains that are generated by the larger Zeolite 4A aggregates.

Table 4. List of SCWF materials produced.

SCWF ID	Salt mass, g	Zeolite mass, g	Zeolite pre-treatment	Salt/Zeolite mass ratio	Glass mass, g	Salt/Glass mass ratio	Thermal Cycle
SCWF-4[a]	0.753	5.251	300 °C 2 h	0.143	4.001	0.188	925 °C 2 h
SCWF-11	0.751	5.251	300 °C 2 h	0.143	4.002	0.188	925 °C 2 h
SCWF-12	1.001	5.008	300 °C 2 h	0.200	4.017	0.249	925 °C 2 h
SCWF-13	0.505	5.509	300 °C 2 h	0.092	4.012	0.123	925 °C 2 h

[a] Made with ERX (LiCl-KCl eutectic) salt in prior work.

Material Sample Preparation

The preparation of SCWF materials for characterization by electron microscopy typically involves the fixing of in epoxy, cutting by low speed saw, and rough grinding and polishing to prepare a fine polished surface for electron microscopy. The cutting and polishing operations were previously performed using absolute ethanol as a lubricant to reduce friction and heat buildup during cutting and grinding operations, as well as clear debris and minimize surface damage. Absolute ethanol is used as a lubricant for these operations due to the relatively lower solubility of chloride salts compared to water. However during the course of the work it was observed that detectable dissolution of the residual chloride phases was still occurring in the excess ethanol used to both cut and polish samples.

While this cannot be avoided during the cutting operation of the wasteform, this prompted a modification in the sample preparation procedures for electron microscopy to exclude the use of ethanol in the polishing procedures. This is achieved by careful dry polishing of cross-sectioned wasteforms in an argon atmosphere glovebox using SiC papers. By using this technique, small halite inclusions may be preserved mostly intact, and surface finishes can be achieved which are suitable for microstructure characterization (<5 micron feature sizes). In this work, the sample of ORX salt, SCWF-12, and SCWF-13 were prepared in this way.

3. RESULTS AND DISCUSSION

3.1 LiCl based SCWF

Material SCWF-11 was made to demonstrate the effect of using a LiCl-based salt chemistry with elevated fission product concentrations to reflect LiCl-based pyroprocessing waste salt which has undergone drawdown and melt crystallization operations to increase active metal fission product concentrations. The materials were processed at 925 °C for 2 h to match the preparation of previous SCWF materials made with LiCl-KCl based salt. Images of the mixture before and after fabrication are shown in Figure 4a and 4b. The crushed and sized reagents are shown mechanically mixed within the crucible, and after processing the wasteform appears to undergo significant consolidation and densification consistent with previous SCWF products. Whereas many of the previous products made with ERX salt pulled away from the walls of the crucible to form a cake-like morphology, this material made with ORX salt flowed to wet the walls of the crucible and fill the available space. While the reason for the different behaviors is not clear, it may be related to the viscosity of the glass due to ion exchange between Na_2O and LiCl to form Li_2O.

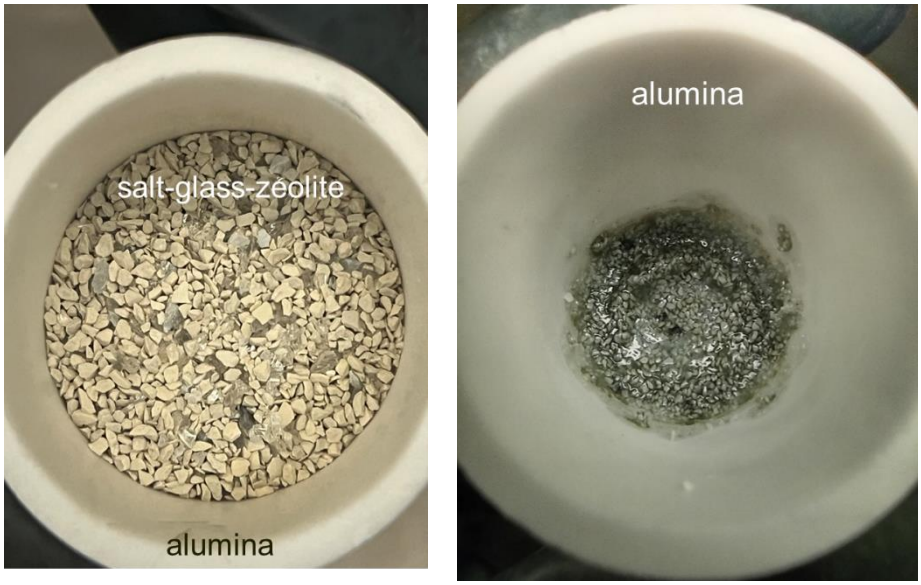

(a) (b)

Figure 4. Photographs of (a) mixed reagents added to alumina crucible and (b) processed SCWF-11 material.

Light optical photograph and BSE micrograph of SCWF-11 are shown in Figure 5. From Figure 5a, the cross section of the wasteform appears well consolidated, but with numerous spherical voids in the microstructure that are < 500 μm in diameter. Prior work with these materials indicated some of the spherical voids are those left by halite inclusions in the structure. The BSE micrograph in Figure 5b of the SCWF-11 microstructure confirms this, demonstrating an identical morphology to previous SCWF materials made with ERX salt. That is, spherical halite inclusions are observed embedded in the binder glass microstructure, in addition to the microencapsulated sodalite grains.

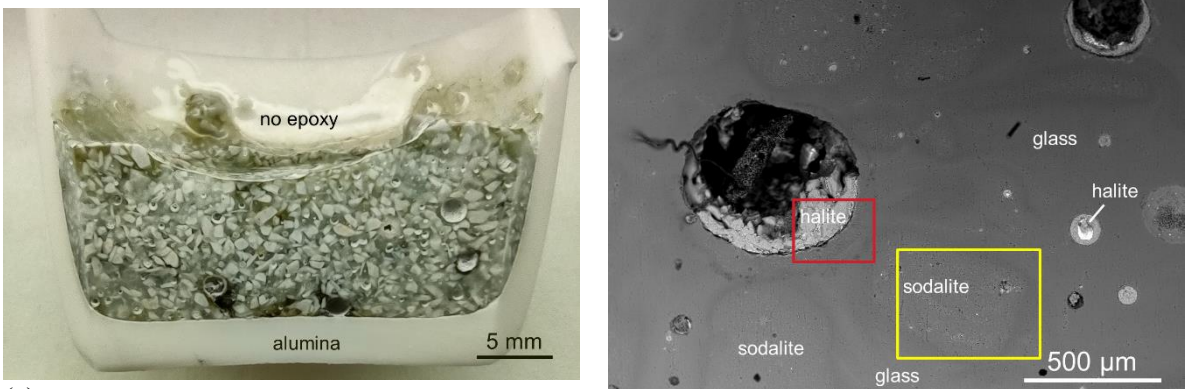

(a) (b)

Figure 5. (a) Optical photo of polished cross section and (b) BSE-SEM photomicrograph of SCWF-11.

Higher magnification BSE imaging of the sodalite domain (yellow boxed region) in Figure 5b is shown in Figure 6. While the contrast between binder glass and sodalite domains is relatively low in the BSE image, sodalite is clearly identified by the EDS maps of Na, Cl and Si in Figure 6b and 6c. The yellow dashed region in Figure 6a is where area-averaged EDS was performed, the results of which are shown in Table 5. This analysis is compared to the stoichiometry for sodalite based on the chemical formula for sodalite. The Cl content from EDS (4.4 at%) agrees well with that expected for sodalite (4.3%). These results indicate that although the salt did not contain NaCl, the Na_2O content of the glass was sufficient to effect the conversion from zeolite to sodalite. Note that the small amount of glass microencapsulating the sodalite grains was included in the EDS analysis.

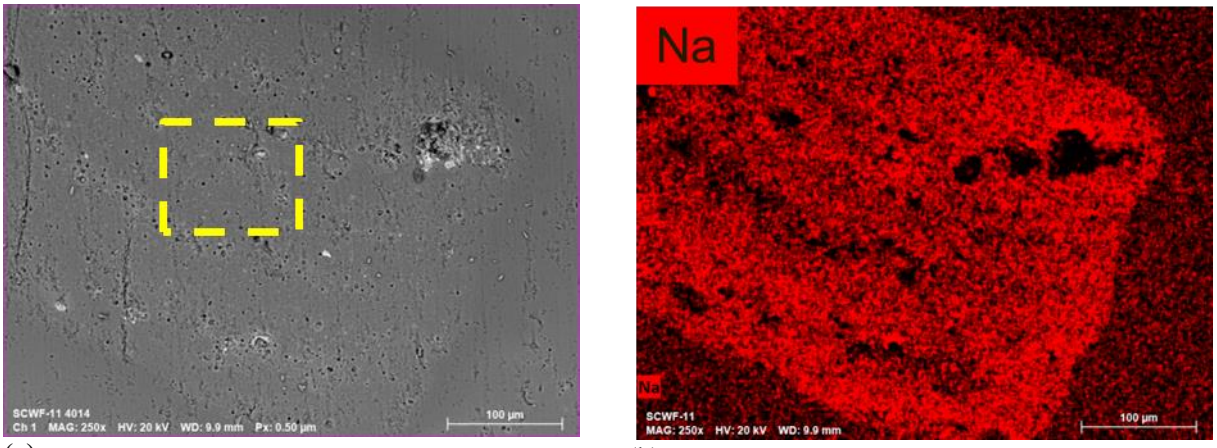

(a) (b)

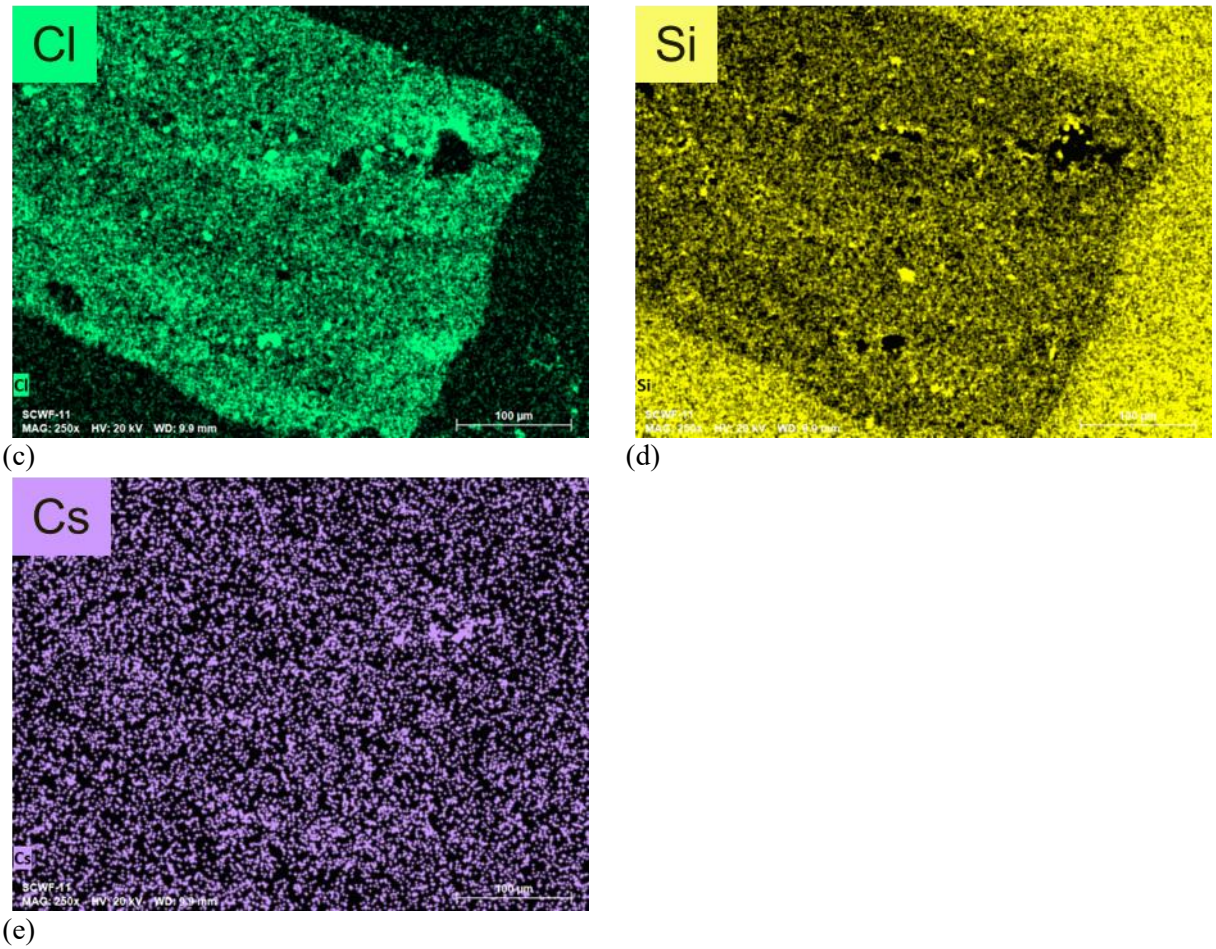

Figure 6. BSE imaging with corresponding EDS maps for a binder-glass encapsulated sodalite grain in SCWF-11 shown in Figure 5. The yellow boxed area in (a) indicates where area-average EDS mapping was performed and is reported in Table 5.

Table 5. Results of area-average EDS mapping in yellow dashed region of Figure 6a, compared to theoretical stoichiometry of sodalite based on the chemical formula in at%.

	O	Na	Mg	Al	Si	Cl	K	Ca	Sr	Cs
EDS	55.3	13.2	0.89	11.5	14.1	4.4	0.1	0.1	0.3	0.2
Sodalite Stoich.	52.2	17.4	-	13.0	13.0	4.3	-	-	-	-

The halite inclusion in the boxed red area of Figure 5 is shown in higher magnification in Figure 7, with corresponding EDS mapping. These results indicate that the halite inclusion consists predominantly of NaCl, but also contains significant Cs content. In comparison to the reagent LiCl salt shown in Figure 3, the overall morphology of dendrite-interdendrite is similar, but the chemistry is significantly different. Notably, from EDS point analysis the dendritic regions are composed of ~40 at% Na and ~50 at% Cl, suggesting substantial ion exchange between the salt and glass phases occurred, where Na migrates from the glass to the salt in exchange for Li. This underscores the NBS4 glass provided substantial Na^+. The interdendrite phase contains up to 6 at% Cs and is likely the consequence of the high Cs content of the reagent salt.

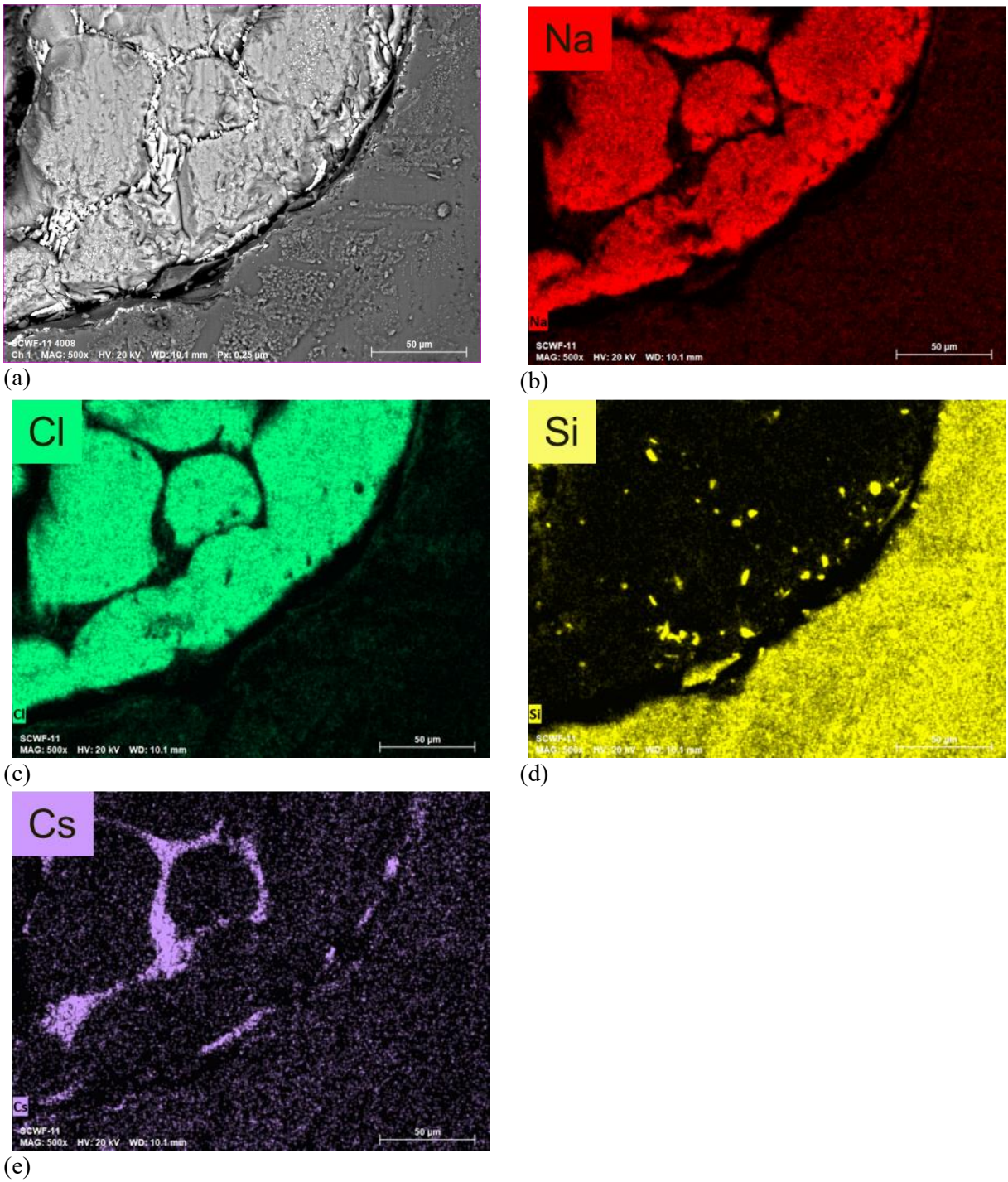

Figure 7. Higher magnification BSE imaging and EDS mapping of the halite inclusion boxed in red in Figure 5b.

The above analyses demonstrate that the SCWF chemistry can be used to immobilize LiCl-based waste salts. High loadings of waste salt with active metal fission products will result in the generation of halite inclusions. Wasteforms are observed to be well consolidated based on cross-sectioned products with little open porosity beyond what can be attributed to halite inclusions. The Na_2O content of NBS4 glass is

sufficient to both facilitate conversion of zeolite to sodalite at this salt loading, as well as effectively ion-exchange with salt constituents. Excess active metal fission products not dissolved in the glass are found predominantly in halite inclusions that are encapsulated in the binder glass rather than in mineral phases such as pollucite.

3.2 Effect of salt content

Materials SCWF-13, SCWF-11, and SCWF-12 compose a series in which the salt content in the CWF was 5, 7.5, or 10 wt% of the total mass of the wasteform reagents. These materials are made with 40 wt% NBS4 glass, and thus are directly comparable to SCWF-4 prepared in the prior SCWF work. Optical photographs of wasteforms synthesized in crucibles and of polished cross sections are shown in Figure 8. In all cases, the wasteforms appear well consolidated from the top-down views, excepting some material which clung to the interior wall of the crucible in SCWF-13 and SCWF-11. Cross sections of each wasteform show relatively dense microstructures with voids from residual halite inclusions which is typical for SCWF chemistries. SCWF-12 exhibits one exception, where at the top surface of the wasteform there appears to be a thin (< 1 mm) white layer visible in the cross section, indicated by a yellow arrow in Figure 8f. In some cases, the wasteform detached from the alumina crucible during sectioning, and consequently the crucible is absent from polished cross-section images.

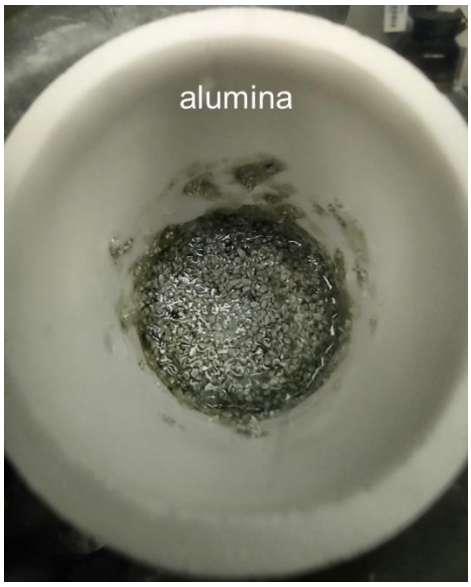

(a)

(b)

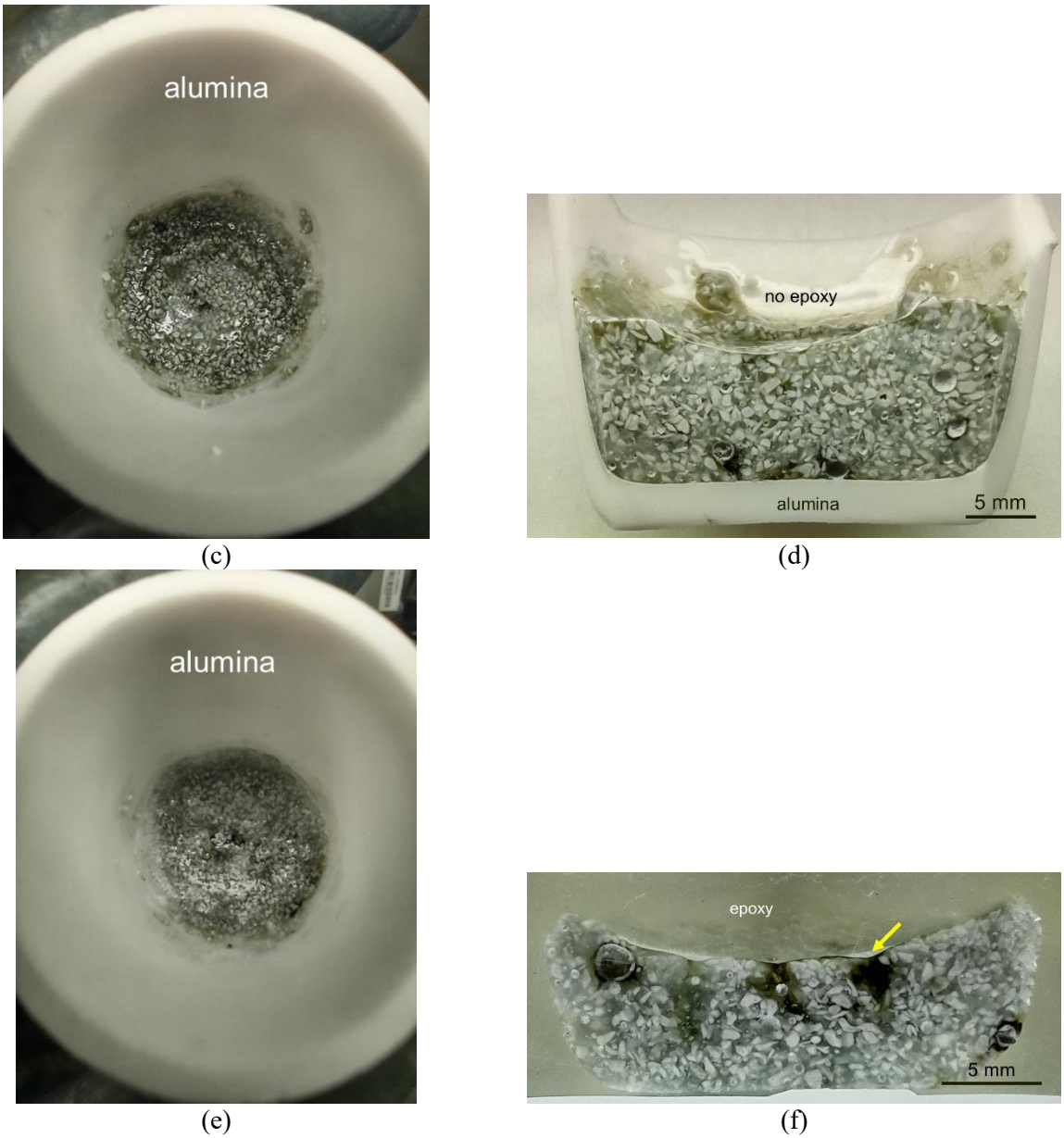

Figure 8. Photographs of materials (a,b) SCWF-13 (c,d) SCWF-11 and (e,f) SCWF-12 with 5, 7.5, and 10 wt% ORX salt respectively.

Sodalite domain characterization

The appearance of sodalite domains and the successful processing as a function of salt content in the wasteform is demonstrated in Figure 9 by BSE imaging and corresponding EDS maps for Cl and Na. In all cases, complete conversion from zeolite to sodalite is observed, indicating the fairly wide range of salt content that the NBS4 glass is able to accommodate and facilitate conversion by provision of Na. The sodalite grains observed in all wasteforms typically appeared as that in Figure 9b, consisting of sodalite grains with the residual clay binder dissolved or encapsulated in the binder glass, or as in Figure 9c, where small halite inclusions were observed within the sodalite grain. Higher magnification BSE imaging and EDS mapping were performed in the yellow boxed region of Figure 9c, which is shown in Figure 10 to

demonstrate the inclusions. From the mapping, the correlation of Na and Cl with these inclusions indicates they are predominantly halite. In these regions are also elevated concentrations of Cs, suggesting that Cs is present in these halite inclusions. These results strongly reinforce the capacity of zeolite to occlude salt during processing, including the active metal fission products, and to form sodalite across all salt loadings tested.

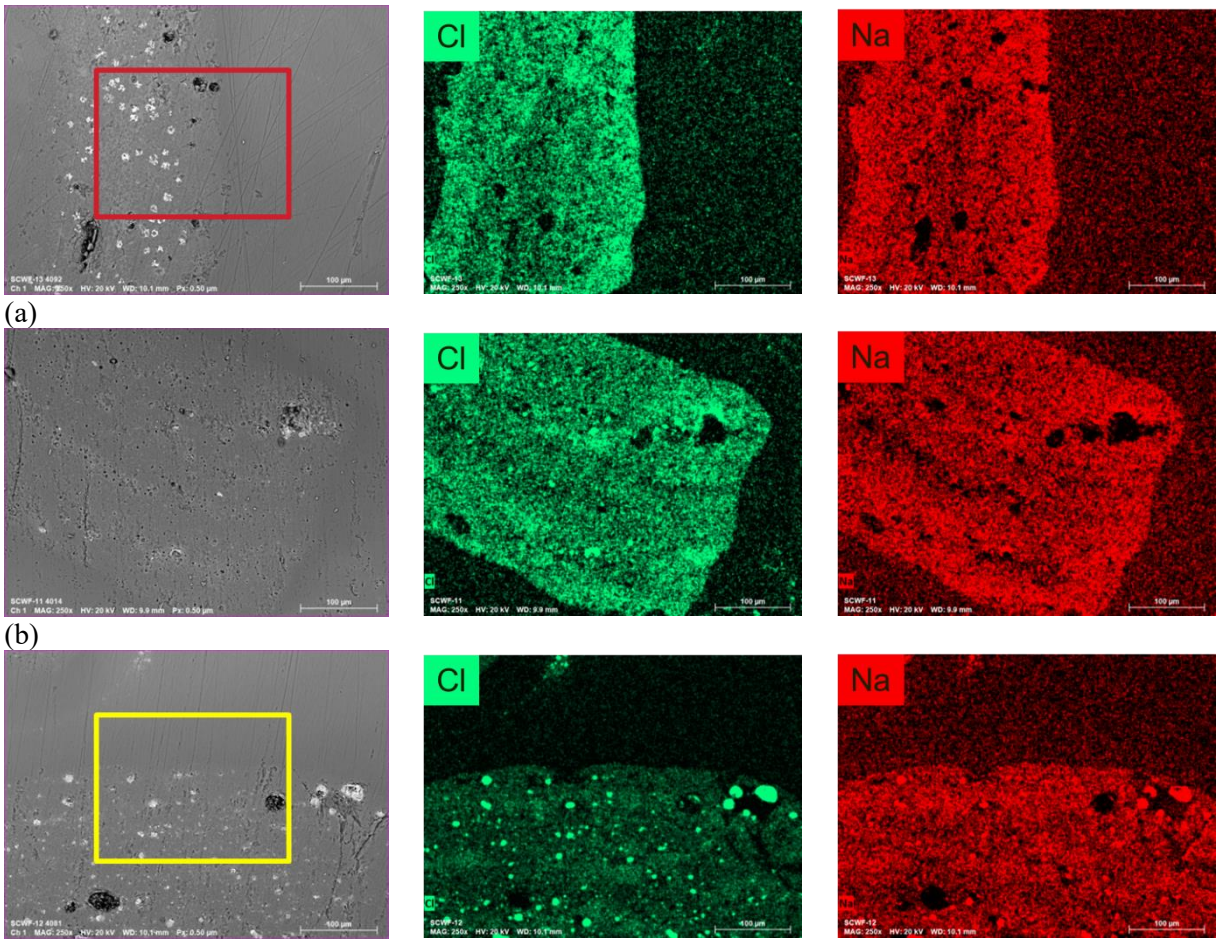

Figure 9: BSE images and corresponding EDS maps for Cl and Na of representative sodalite grains in (a) SCWF-13 made with 5% salt, (b) SCWF-11 made with 7.5% salt, and (c) SCWF-12 made with 10% salt.

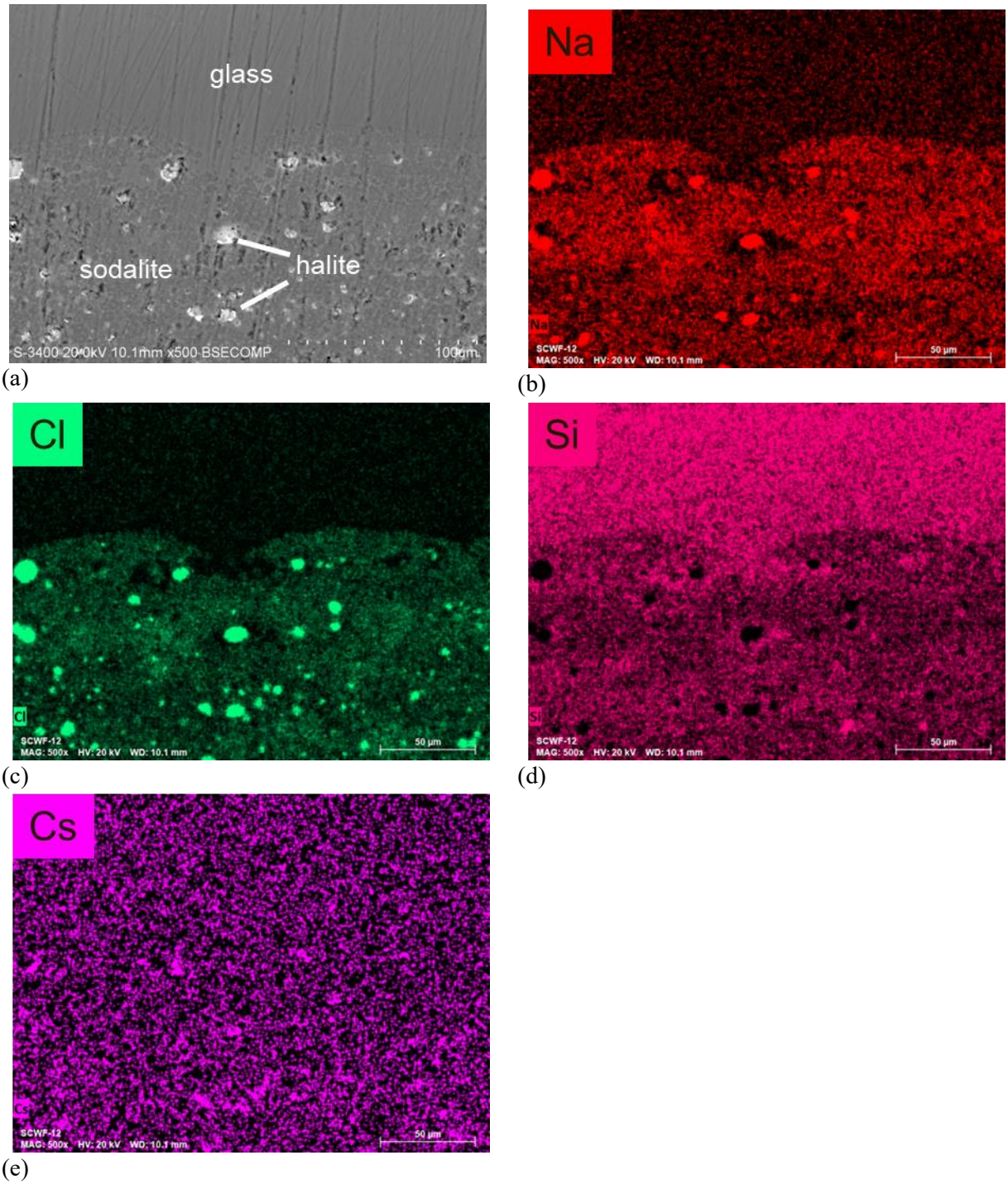

Figure 10. BSE imaging and corresponding EDS mapping of a sodalite domain in SCWF-12 which demonstrated halite inclusions in the sodalite.

In SCWF-13 made with the lowest salt loading of 5 wt%, a relatively low number of sodalite grains appeared such as shown in Figure 9a, containing bright inclusions by BSE which do not correlate with Cl or Na mappings, suggesting they are not halite inclusions. High magnification BSE imaging was performed in the red boxed area indicated in Figure 9a and is shown in Figure 11. Analysis in this region indicates that

these inclusions are rich in Cs. Comparison to the work of Lambregts and Frank published in 2003 (Lambregts 2003) where they formulated ceramic wasteforms with 25, 50, 75, and 100% CsCl (in NaCl) indicates a similar morphology of the phases in Figure 11a to the Cs-pollucite ($Cs_2Al_2Si_4O_{12}$) within sodalite domains that they had observed. Furthermore, the inclusions are located between grains of the sodalite-converted zeolite, rather than in the sodalite itself or in the bulk glass binder, where residual clay binder is expected to be present. It is reasonable to assume that the combination of higher fission product loading and also the lower salt content of the wasteform may, in some isolated cases in the wasteform, encourage the formation of Cs-rich oxide phases in the microstructure. Sodalite domains with Cs-pollucite were infrequently detected in the microstructure, however.

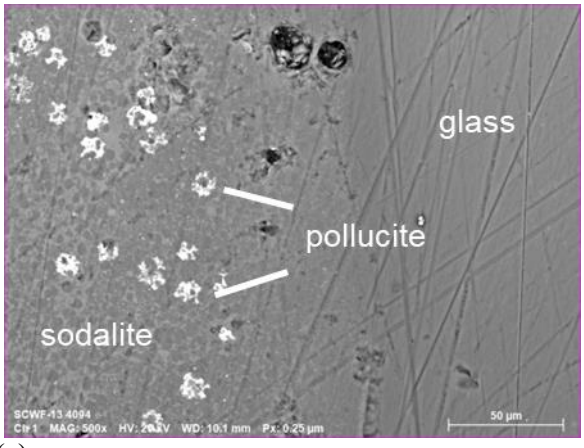

(a)

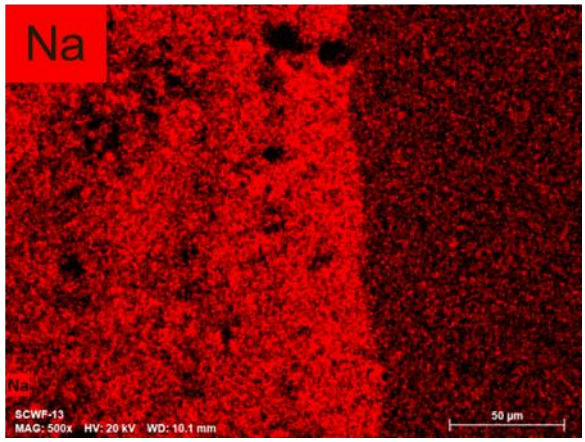

(b)

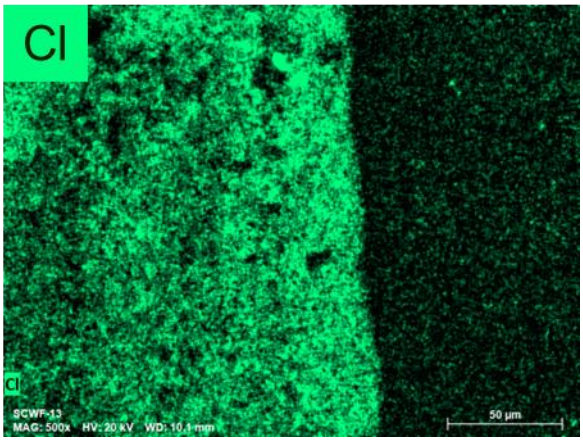

(c)

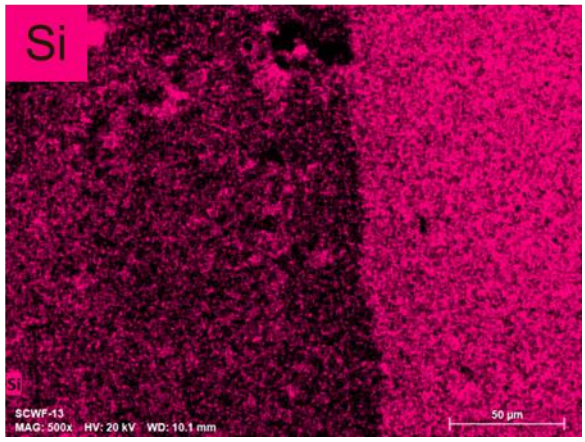

(d)

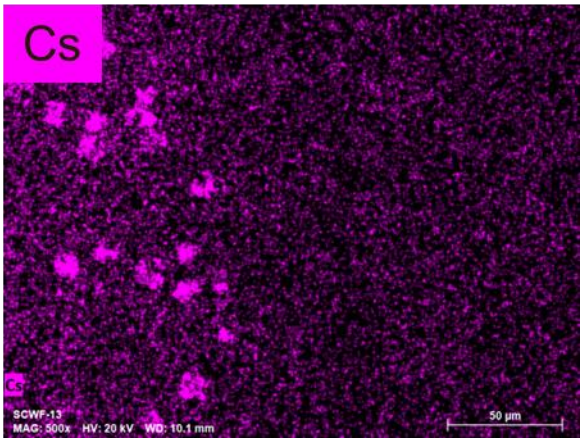

(e)

Figure 11. BSE imaging and corresponding EDS mapping of a sodalite domain in SCWF-13 which demonstrated Cs-rich inclusions in the zeolite binder which is likely Cs-pollucite ($Cs_2Al_2Si_4O_{12}$).

Halite inclusion characterization

The morphology of halite inclusions across all salt loadings tested was examined by SEM-EDS, for which BSE images and corresponding Na and Cs mappings are shown in Figure 12. These results indicate that across all salt loadings tested, halite inclusions appear to have similar chemistry and morphology: they consist predominantly of NaCl and also contain Cs in the isolated phase which appears brighter by BSE imaging due to the high atomic number of Cs. While the binder glass shows good capacity to encapsulate these salt phases, excess halite phase was found at the surface of the wasteform for SCWF-12 with the highest salt loading (10 wt%).

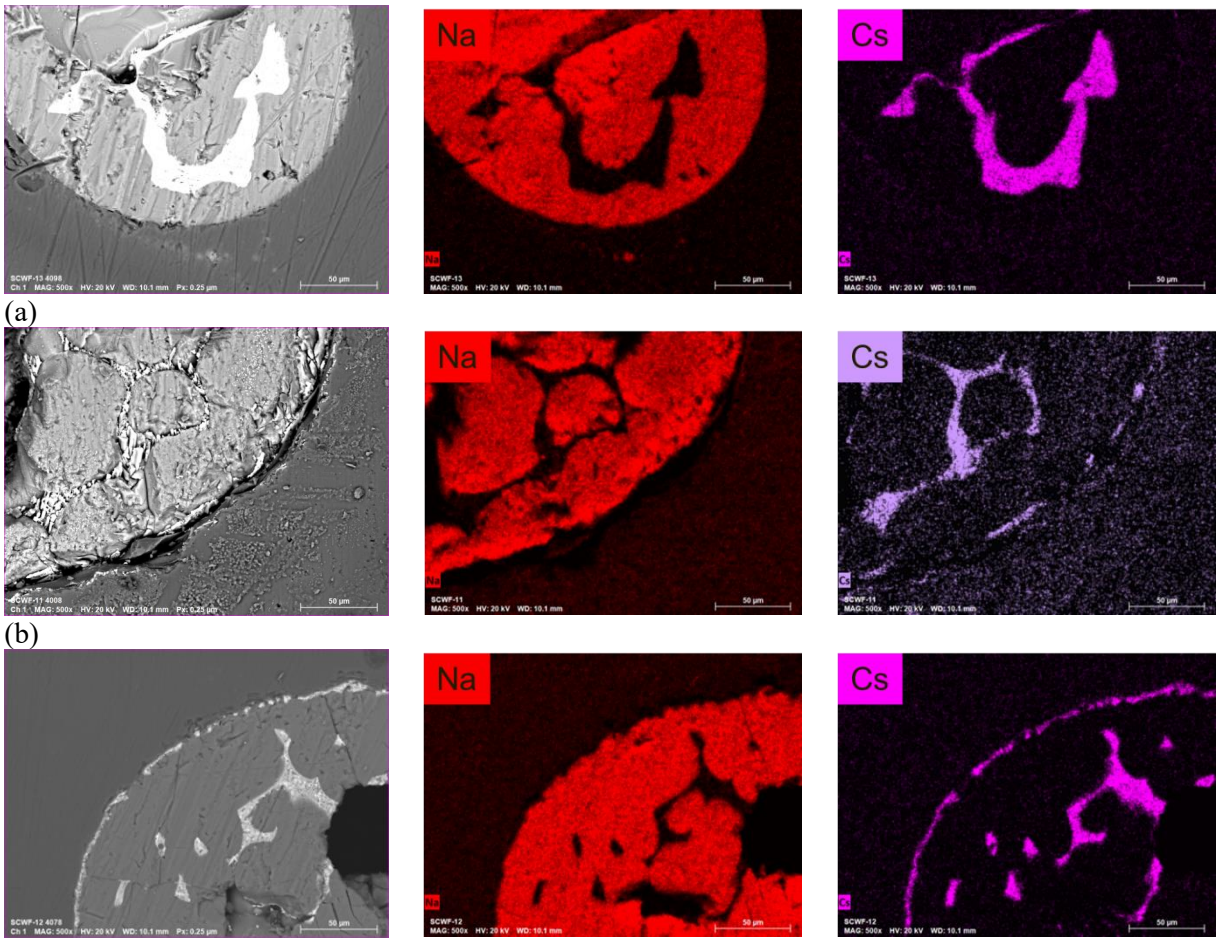

Figure 12. BSE imaging and corresponding EDS mapping of halite domains in (a) SCWF-13, (b) SCWF-11, and (c) SCWF-12 which demonstrate encapsulation of halite within the glass binder, along with excess Cs.

This region is indicated by the yellow arrow in Figure 8f, for which higher magnification BSE imaging and corresponding EDS maps are shown in Figure 13. This shows a roughly 100-300 µm thick film of

halite on the surface of the wasteform. Its morphology and location suggests this is the result of density based separation of salt from the glass binder during processing (lower density halite accumulating on the surface). This is an indication that the maximum amount of LiCl-based salt that can be incorporated into the waste form either in sodalite, dissolved in the glass, or in halite inclusions in the glass or sodalite domains is less than 10 wt%. Prior work on the ACWF determined the acceptable LiCl-KCl salt loading to be approximately 11 wt% (Ebert, 2016). In comparison to these results, it suggests a lower salt loading is necessary to prevent the density-based separation of salt from the wasteform.

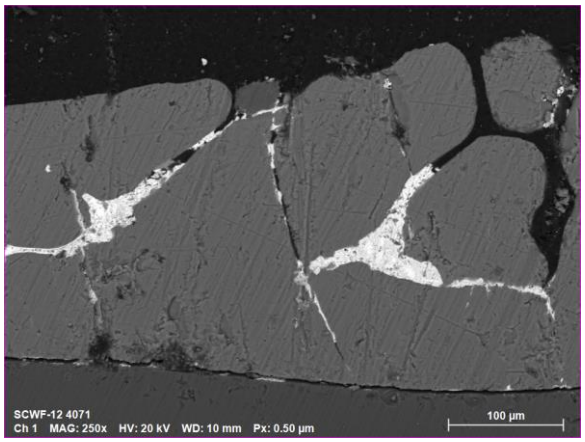

(a)

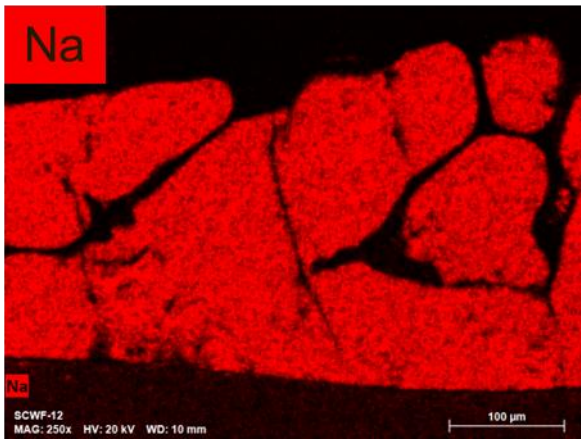

(b)

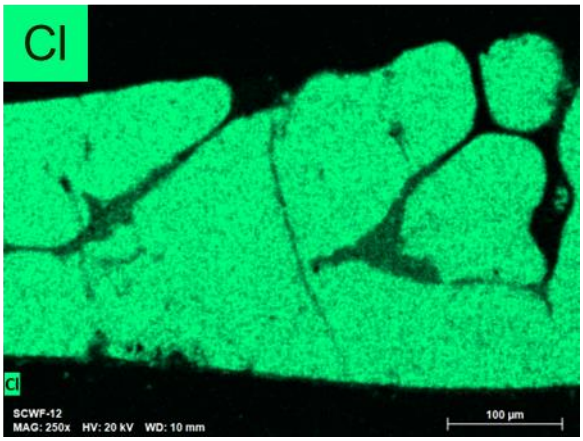

(c)

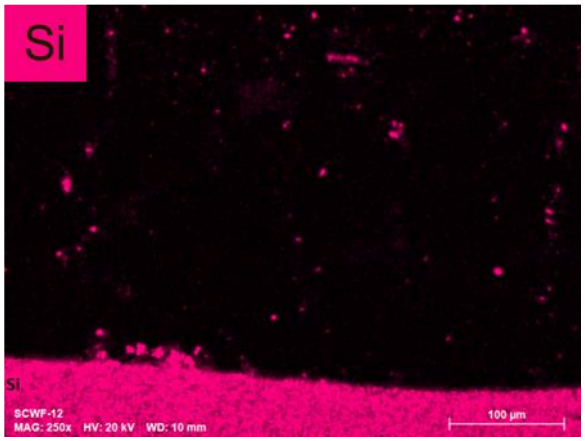

(d)

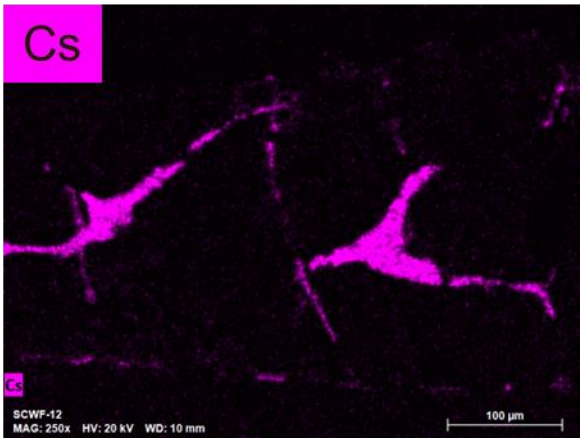

(e)

Figure 13. BSE imaging with corresponding EDS mapping of the area indicated by the yellow arrow in Figure 8f, showing a layer of excess salt on the surface of SCWF-12 (10 wt% ORX salt) which likely separated out due to the lower density of salt liquid.

3.3 Degradation Behavior

The ASTM C1308 test method (ASTM 2025a) has been routinely used to measure the intrinsic dissolution rates of CWF materials under highly dilute conditions. The test responses are very sensitive to the relative amounts, compositions, and stabilities of the phases comprising the SCWF materials. The ASTM C1308 test provides a rapid means of comparing different materials based on the intrinsic behaviors of constituent phases under dilute far-from-equilibrium conditions. That is, saturation effects that will control long-term degradation behavior in a disposal facility are intentionally avoided by using the test method. In this case, the test is conducted to discriminate dissolution behaviors of highly soluble halite, moderately soluble glass, low solubility sodalite phases formed in different SCWF materials. The test is conducted by immersing a specimen with known surface area and gross composition in a large volume of demineralized water to achieve a low specimen surface area-to- solution volume ratio, heating at 90 °C, and completely exchanging the solution with fresh water every 24 hours. The solution concentrations of key elements are measured at each exchange and used to quantify the mass of the specimen dissolved. The slopes of plots of the cumulative releases of key elements over cumulative duration normalized to the specimen surface area and mass fraction of each element in the SCWF material provide a measure of the intrinsic dissolution rate of the material as the average over the last three test intervals. The measured solution concentrations represent the combined dissolution of all phases and can be deconvolved based on the phase compositions and examination of the reacted surface to identify preferentially dissolved phases. The concentrations measured after the first interval are dominated by dissolution of highly soluble salt inclusions and are affected by sample preparation (e.g., roughness, fracturing, residual debris). The *y*-intercepts of the plots represent the amounts that dissolved rapidly during the first test interval. Concentration measured after the three following intervals are dominated by dissolution of sodalite, binder glass, and any salt inclusions that became exposed during the interval. The average of release rates during the second, third, and fourth intervals are used to represent the intrinsic material durability; the average is given by the slope of the regressed line.

The measured solution concentrations are normalized to the estimated geometric surface area of the waste form exposed at the surface of the polished cross section (the entire mount was immersed) and the element mass fractions calculated from the amounts and compositions of Zeolite 4A, NBS4 glass, and salt used to synthesize the material. Test results are evaluated in terms of the normalized elemental mass loss values calculated for each test interval (i.e., after each solution exchange). The normalized elemental mass loss function NL(i) utilizes the concentration of a soluble element *i* measured in the test solution to represent the mass of the material being tested that had dissolved (in this case, the multiphase SCWF material). The NL(i) values calculated using different species are used to differentiate dissolution of sodalite, glass, and salt phases. The dissolved mass is normalized to the geometric surface area of the test specimen to provide a value that can be used to compare tests with different specimen areas. Dissolution occurring in each interval of a test series is referred to as the incremental normalized mass loss and is calculated as

$$incremental\ NL(i) = \frac{C(i)_n}{S/_V f(i)}, \quad (2)$$

where $C(i)_n$ is the concentration of species *i* measured in the test solution during test interval *n*, *S* is the geometric surface area of the test specimen, *V* is the volume of test solution, and $f(i)$ is the mass fraction of species *i* in the CWF or ACWF material used in the test. Values of NL(i) are presented as g m^{-2} and represent the mass of SCWF material that dissolved during the test interval, not the masses of individual species *i*

that have been released. These values allow for direct comparisons of materials having different compositions (i.e., materials made with different amounts of binder glass, Zeolite 4A, and salt) in tests conducted at different S/V ratios and with different exchange intervals. For the ASTM C1308 tests, the cumulative dissolution occurring through a series of n test intervals is calculated as the sum of the n incremental $NL(i)_n$ values as

$$cumulative\ NL(i) = \sum NL(i)_n = \sum \frac{C(i)_n}{S/V f(i)}, \quad (3)$$

It is important to remember that the cumulative value determined in a series of intervals in an ASTM C1308 test includes the effect of exchanging the solution with fresh water and does not account for the solution feedback effects of the cumulative solution. It does include the cumulative effect of surface degradation on the exposed areas of constituent phases during each interval, which could increase or decrease during the test. Also, NL(i) values represent the mass of CWF that was dissolved assuming the entire specimen is composed of phases bearing element i. Therefore, comparing NL(i) values calculated with different element concentrations gives insights into the relative dissolution behaviors of constituent phases.

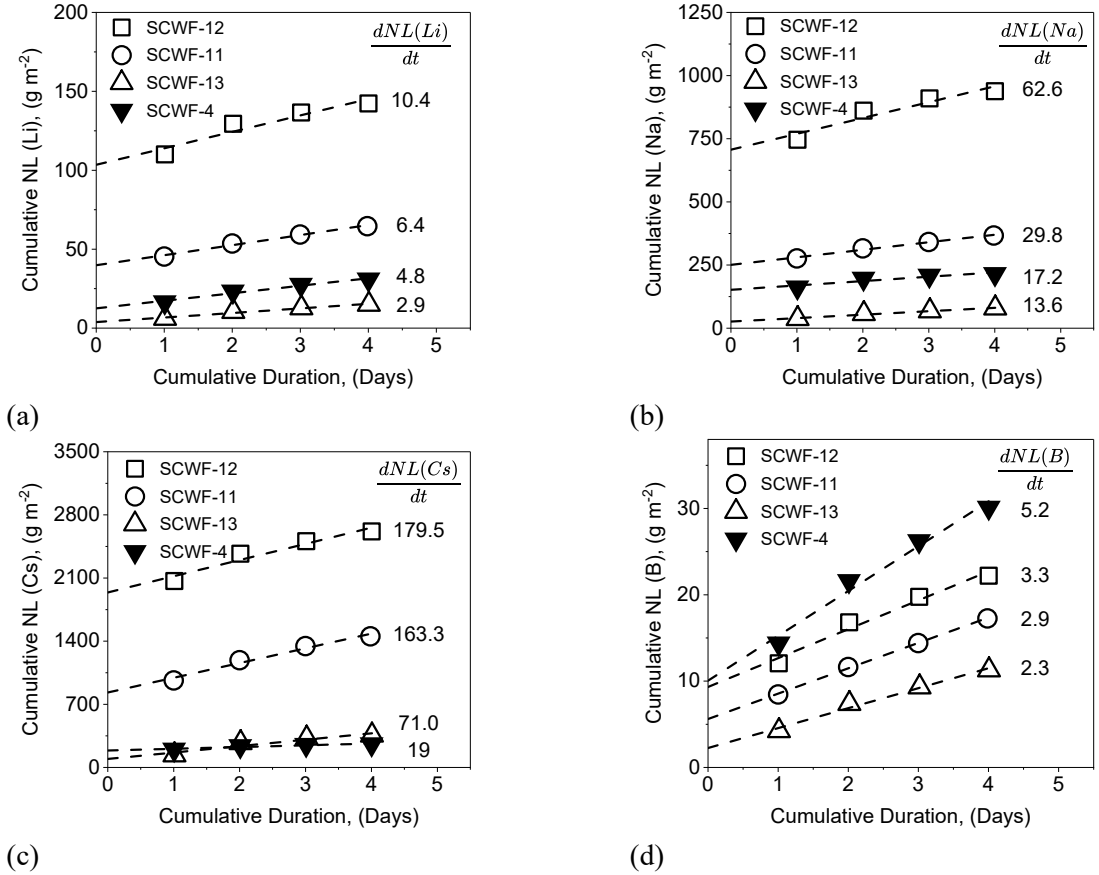

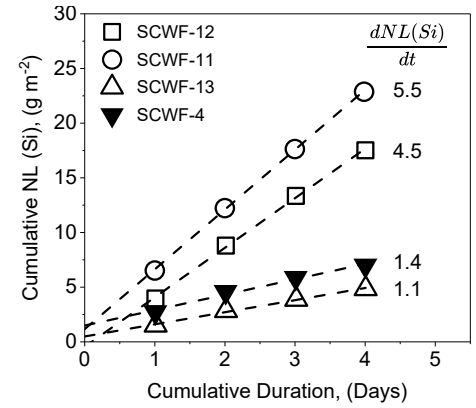

(e)

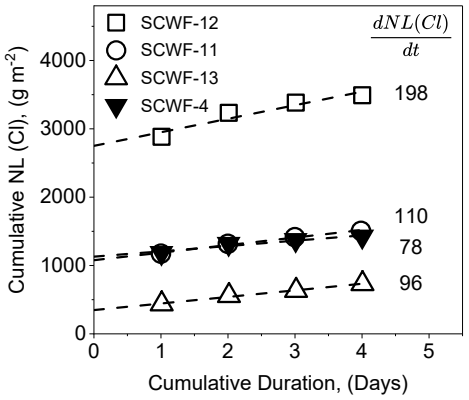

(f)

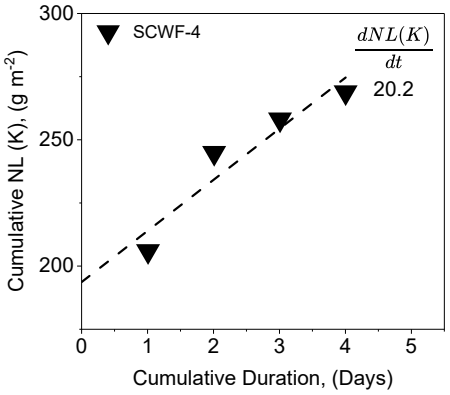

(g)

Figure 14: Cumulative release data for SCWF-4, SCWF-11, SCWF-12, and SCWF-13 (made with 7.5, 7.5, 10, 5 wt% salt, respectively) for (a) Li, (b) Na, (c) Cs, (d) B, (e) Si, (f) Cl, and (g) K for SCWF-4 only. Dashed lines represent linear fits of the data.

Halite release behavior

Figure 14 summarizes ASTM C1308 results for SCWF-11, SCWF-12, SCWF-13 (ORX salt) and SCWF-4 (ERX salt) for direct comparison . For the ORX materials, the first interval values for NL(Li), NL(Na), NL(Cs), and NL(Cl) in Figure 14a, 14b, 14c, and 14e indicate the initial releases are directly correlated to the salt content of the waste form, consistent with a larger fraction of readily accessible salt phases generated in materials with higher salt contents. For example, the initial release of Na increases with increasing salt loading (5 wt%, 7.5 wt%, 10 wt%, SCWF-13, SCWF-11, and SCWF-12 respectively). This is consistent with fixed amounts of sodalite and binder glass in the three materials and more halite inclusions being formed in materials made with higher salt contents. The releases in the subsequent intervals are fairly constant.

SCWF-4 contained 7.5 wt% of salt and its initial release behavior is intermediate between those of SCWF-13 and SCWF-11 for NL(Li), NL(Na), and NL(Cs) in Figure 14 a, 14b, and 14c. However, from Figure 14e, the initial release for NL(Cl) suggests that a similar quantity of salt inclusions was also present in SCWF-11 at 7.5 wt% salt loading. The apparent differences in Li, Na, and Cs are probably a consequence of their partitioning between glass and halite phases. However, for NL(Na), the cause for elevated Na content in the initial release for SCWF-11 compared to SCWF-4 (276 vs. 161 gm^{-2}) is not immediately obvious, assuming the majority of the initial release for Na emerges from the dissolution of

halite. This may be related to the KCl content of the LiCl-KCl salt used to make SCWF-4 which offsets the quantity of NaCl formed by ion exchange with the glass. The dissolution rate of SCWF-4 based on NL(K) was 20 gm^{-2}, similar to that of SCWF-11 based on NL(Na).

Salt-glass interaction

All of the sodalite and halite in SCWF-11 was generated by reactions with NaCl formed from the exchange of Na in the glass for alkali metals from the salt, dominated by lithium. Observation of slightly higher NL(Na) values in the test with SCWF-11 compared to the test with SCWF-4 suggests a higher affinity of Li (compared to Na or K) for the glass phase than in the salt phase, resulting in more NaCl generated in SCWF-11 than in SCWF-4. This is supported by calculation of the overall change in standard Gibb's free energy (ΔG°) for the reactions $2Li + 0.5O_2 = Li_2O$ vs. $2Na + 0.5O_2 + Na_2O$ (-439 vs. -250 kJ at 925 °C) presented in Table 6. The initial release for K is more than one order of magnitude higher than the initial release for Li (16.4 gm^{-2}) in SCWF-4. Calculation of ΔG° for $2 K + 0.5 O_2 = K_2O$ (-179 kJ at 925 °C) similarly suggests the affinity of Li for the glass phase is greater than that of K. Therefore, exchange of Li in the salt with Na in the glass is expected to be dominant when processing either ORX or ERX waste salt.

Table 6. Calculated change in standard Gibbs free energy (ΔG°) for formation of select active metal oxides at 925 °C (1198 K) from thermochemical database (Bale, 2016).

Reaction Formula	ΔG° (kJ)
$2 Li + 0.5 O_2 = Li_2O$	-439
$2 Na + 0.5 O_2 = Na_2O$	-250
$2 K + 0.5 O_2 = K_2O$	-179
$2 Cs + 0.5 O_2 = Cs_2O$	-163
$Sr + 0.5 O_2 = SrO$	-472

The suggestion of changes in chemistry due to thermodynamically driven ion exchange is supported by the results of ICP-MS analysis of the initial release solutions (Day 1) which are not normalized to the mass of the element in the CWF product. Shown in Table 7, weight percentages of dissolved elements were calculated from the measured concentration of a given cation (C_i) in µg/L, divided by the summed concentrations of all cations in that solution ($(C_i / \sum_i^j C_i) \times 100\%$). These results indicate that for SCWF-13, SCWF-11, and SCWF-12 with 5, 7.5 and 10 wt% ORX salt as well as SCWF-4 with 7.5 wt% ERX salt, the majority of cations in the initial test solution were Na, with very little Li relative to the high content in the added waste salt. This suggests that during the waste form processing, almost all of the LiCl in the salt phase exchanges for Na_2O in the glass to form NaCl (assuming the majority of Na in solution comes from halite dissolution and not sodalite dissolution). This also indicates that the Cs content is relatively high in the halite phase, which is consistent with microstructure observations of halite inclusions in Figure 12. This is likely related to the lower affinity of Cs for the glass phase compared to Li suggested by standard Gibbs free energy calculations in Table 6 (-163 vs. -439 kJ).

Table 7. Concentration of cations from ICP-MS analysis of ASTM C1308 test solutions taken after the first day of immersion for each CWF, in wt%.

	Li	B	Na	Al	Si	K	Sr	Cs	Nd
SCWF-12	1.1%	0.1%	85.9%	0.0%	0.7%	0.0%	0.1%	12.0%	0.0%
SCWF-11	0.9%	0.2%	84.7%	0.2%	3.0%	0.0%	0.2%	10.9%	0.0%
SCWF-13	0.6%	0.7%	84.9%	1.1%	5.1%	0.0%	0.1%	7.5%	0.0%

SCWF-4	0.2%	0.6%	82.7%	0.4%	2.0%	12.1%	0.0%	2.0%	0.0%

Binder glass degradation behavior

As B is exclusive to the borosilicate glass phase, the influence of waste salt composition on the binder glass degradation is directly indicated by the results for NL(B) in Figure 16c. The slope of cumulative release with respect to cumulative duration ($dNL(B)/dt$) increases slightly with increased ORX salt loading (2.3, 2.9, 3.3 $gm^{-2}d^{-1}$), which suggests there may be some small increase in the degradation rate of the binder glass as salt loading increases. This suggests that the increased Li content (and subsequently Li_2O in the binder glass after ion exchange) does not result in a substantially increased rate of glass degradation. However, the test with SCWF-4 shows the highest release rate (5.2 $gm^{-2}d^{-1}$) based on NL(B). This suggests that the glass phase formed in waste forms made with ORX salt is slightly more durable than that formed in CWF made with ERX salt.

Sodalite domain degradation behavior

The influence of LiCl salt on the degradation rate of sodalite domains is indicated from the results of NL(Cl), NL(Si), and NL(Na). Comparison of $dNL(Cl)/dt$ results for SCWF-4 and SCWF-11 indicates a higher value from 78 to 110 $gm^{-2}d^{-1}$ due to the change in salt chemistry of the waste form. As additional chloride release after the first day of testing likely arises from sodalite degradation rather than continued halite dissolution, this indicates that there may be some increase in the extent of sodalite degradation due to the change in salt chemistry. The release rate based on Si ($dNL(Si)/dt$) increases significantly with ORX salt loading (namely, 1.1 at 5 wt%, 4.5 at 10 wt%, and 5.5 $gm^{-2}d^{-1}$ at 7.5 wt%). As Si is common to both the glass binder and the sodalite domain (sodalite and the clay binder), this may suggest that above a specific salt loading (at least 5 wt%), the LiCl salt may increase the rate of sodalite degradation.

This increased rate of sodalite domain degradation may be more clearly indicated by the relative increase in slope of NL(Na). For example, $dNL(Na)/dt$ increases substantially with increased salt loading (13.6, 29.8, 62.6 $gm^{-2}d^{-1}$), almost doubling with each stepped increase from 5, to 7.5, to 10 wt%. Release of Na which is the result of halite dissolution should be minimal after the first day of testing after the solution is exchanged, due to the high solubility of NaCl in water. Release of Na resulting from the dissolution of the glass binder should overall decrease as salt loading increases, due to the decreasing concentration of Na in the glass due to ion exchange with Li. This then suggests that the increased release rate for Na is more likely due to increased dissolution of sodalite.

This is similar for $dNL(Li)/dt$, which increases with increasing salt loading (2.9, 6.4, 10.4 $gm^{-2}d^{-1}$), suggesting increasing salt content also increases the glass phase dissolution rate. These values are significantly lower than those for $dNL(Na)/dt$, which include dissolution of the sodalite domains. It may be the case that the elevated LiCl concentration in the reagent salt, in combination with the increased salt loading, drives forward the formation of lower durability phases within sodalite domains. This may be ultimately reflected in the release rate for Cs, $dNL(Cs)/dt$, which nearly doubles from 5 wt% to 7.5 wt% (71, 163 $gm^{-2}d^{-1}$) and may plateau at 10 wt% (179 $gm^{-2}d^{-1}$). These results indicate that increasing the quantity of LiCl based salt within the waste form thus increases the Cs uptake within the sodalite domains, likely into the clay binder due to the exclusivity of sodalite for Na. This also substantially increases the initial release rate of Cs due to the formation of excess halite, and also increases the degradation rate of the sodalite domains (sodalite and clay binder).

These above effects that have been discussed are strongly coupled to the salt chemistry. Directly comparing results for SCWF-4 vs. SCWF-11 that have the same salt loadings and glass content, the change from LiCl-KCl eutectic to LiCl based waste salt decreases the glass phase dissolution rate based

on NL(B) (5.2 vs. 2.9 $gm^{-2}d^{-1}$). While Cs and Sr content were increased by a factor of 3 in the ORX salt compared to the ERX chemistry (Table 1), using LiCl based salt increases the initial NL(Cs) values (198 vs. 964 gm^{-2}) and release rate based on NL(Cs) (19 vs. 163 $gm^{-2}d^{-1}$) by more than a factor of 3, in excess of the proportion by which the chemistry was modified. This also increases the initial release (161 vs. 275 gm^{-2}) and release rate based on NL(Na) (17.2 vs. 29.8 $gm^{-2}d^{-1}$) despite no NaCl being added to the LiCl based chemistry. While the mechanism underlying these observations is not clear from this data, it may be due to the affinity of the Li cation for the glass phase. Similar to the analysis for Na and K, the change in standard Gibbs free energy for formation of Cs_2O is less negative than for Li_2O (-163 vs. -439 kJ). The increased Li content of the glass may then prevent relatively lower affinity cations such as Cs from being incorporated into the glass, resulting in disproportionate release and release rates. While this improves the durability of the binder glass, it inhibits the stabilization of other salt constituents in the glass and increases their concentrations in halite by-product inclusion phases. From the data, these effects can be overall mitigated by decreasing the salt loading to below 7.5 wt%.

Post-corrosion microstructure analysis

Microstructure analyses of the waste forms before and after ASTM C1308 testing are shown in Figure 15. In all cases, BSE imaging demonstrates that the initial degradation of the waste form proceeds primarily by dissolution of the sodalite domains rather than of the binder glass phase under the dilute ASTM C1308 test conditions. The pock-marked appearance of the reacted sodalite domain confirms that the sodalite grains were less durable than intergranular glass or bulk glass. This is indicated by the changes in contrast of the sodalite domain, as well as pronouncement of the boundary between the glass and the sodalite domain. Polishing scratches across glass and sodalite regions prior to testing are seen to remain on the glass surface after the tests, but not on in the sodalite domains.

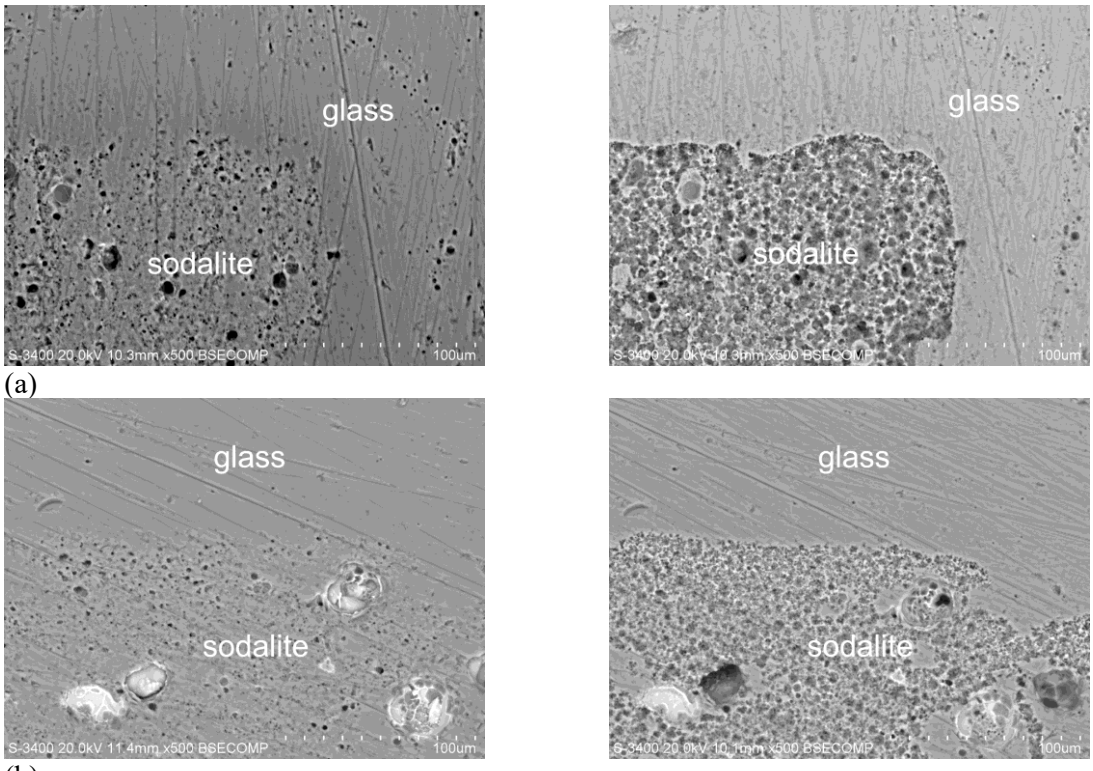

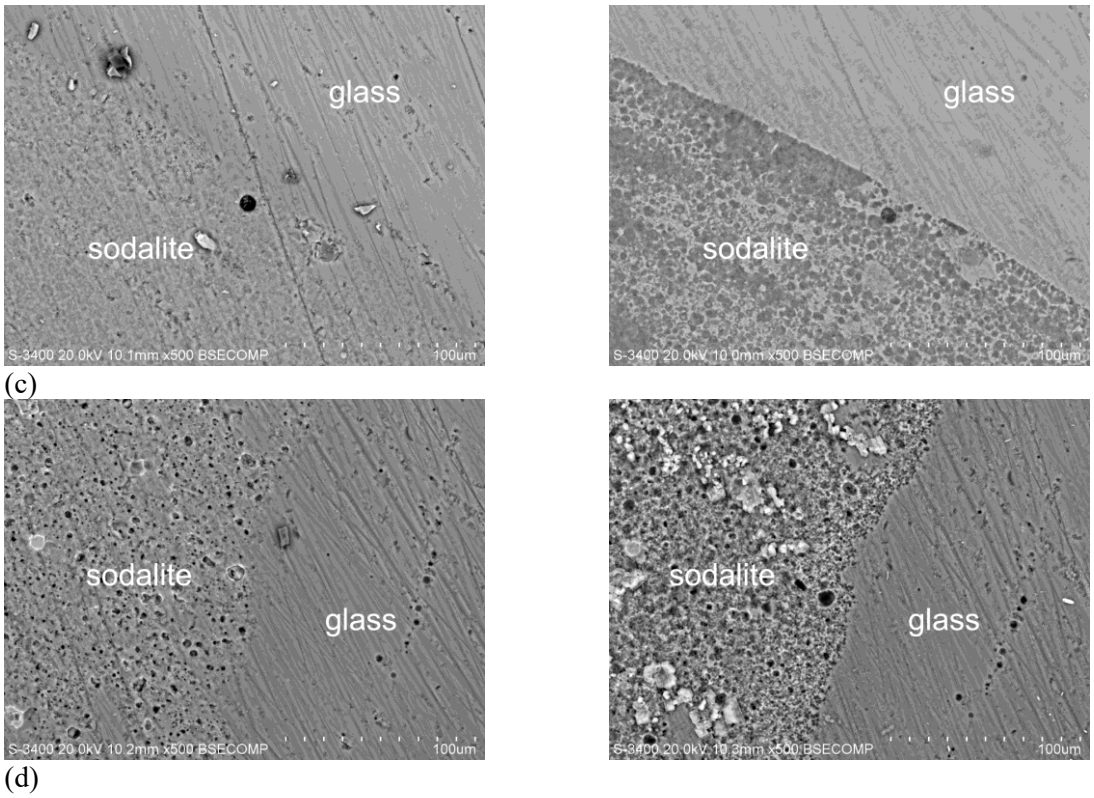

Figure 15: BSE micrographs of (a) SCWF-4, (b) SCWF-13, (c) SCWF-11, and (d) SCWF-12 before (left) and after (right) ASTM C1308 testing.

The EDS mappings of the SCWF-4 surface before and after ASTM C1308 testing shown in Figures 16a and 16b, respectively, show a significant relative decrease in the Na content of the sodalite domain compared to the bulk glass due to dissolution of sodalite grains. The glass between grains remains. While the relatively low Cs content makes EDS point analysis difficult to quantify Cs content, mapping for Cs shows no apparent change after the sodalite grains dissolved. Mapping of SCWF-12 before testing shows a similar chemical distribution to SCWF-4, however after ASTM C1308 testing the mapping for Na indicates the reprecipitation of NaCl evaporites onto the wasteform surface. Mapping for Cs does suggest an increase in the average Cs content of the sodalite domains after the sodalite grains dissolved during testing. As dissolution of the sodalite grain occurs preferentially to the glass, this mapping suggests Cs-rich domains within the sodalite domain are more durable than the sodalite grains, resulting in their increased concentration (lower durability phases dissolving faster than higher durability phases).

Considering the observations of Cs-pollucite in Figure 11 in SCWF-13 (5 wt% salt), it may be the case that at high and low salt loadings, the elevated Cs content of the salt drives Cs into other phases by two distinct mechanisms. The first mechanism at low salt loadings may be due to the consumption of NaCl by zeolite to form sodalite, which forces the remaining cations to enter an oxide phase (either NBS4 glass, or clay binder). The second mechanism at high salt loadings is likely the result of the affinity of Li for the glass phase, which pushes larger cations such as Na and Cs into other phases. This likely correlates with the observation within ASTM C1308 solution analysis of increased Cs initial releases and release rates for the highest salt loading (SCWF-12) in Figure 14c. That is, doubling the salt content from 5 wt% to 10 wt% results in an increase in initial NL(Cs) values in excess of an order of magnitude (137 vs. 2066 g m^{-2}), rather than just doubling. This is probably because the fixed amounts of added zeolite and glass become occupied by more NaCl and Li and cannot accommodate the Cs. In contrast, the release rate

based on NL(Cs) roughly doubles between materials made with 5 wt% and 10 wt% salt loading (71 vs. 179 $gm^{-2}d^{-1}$).

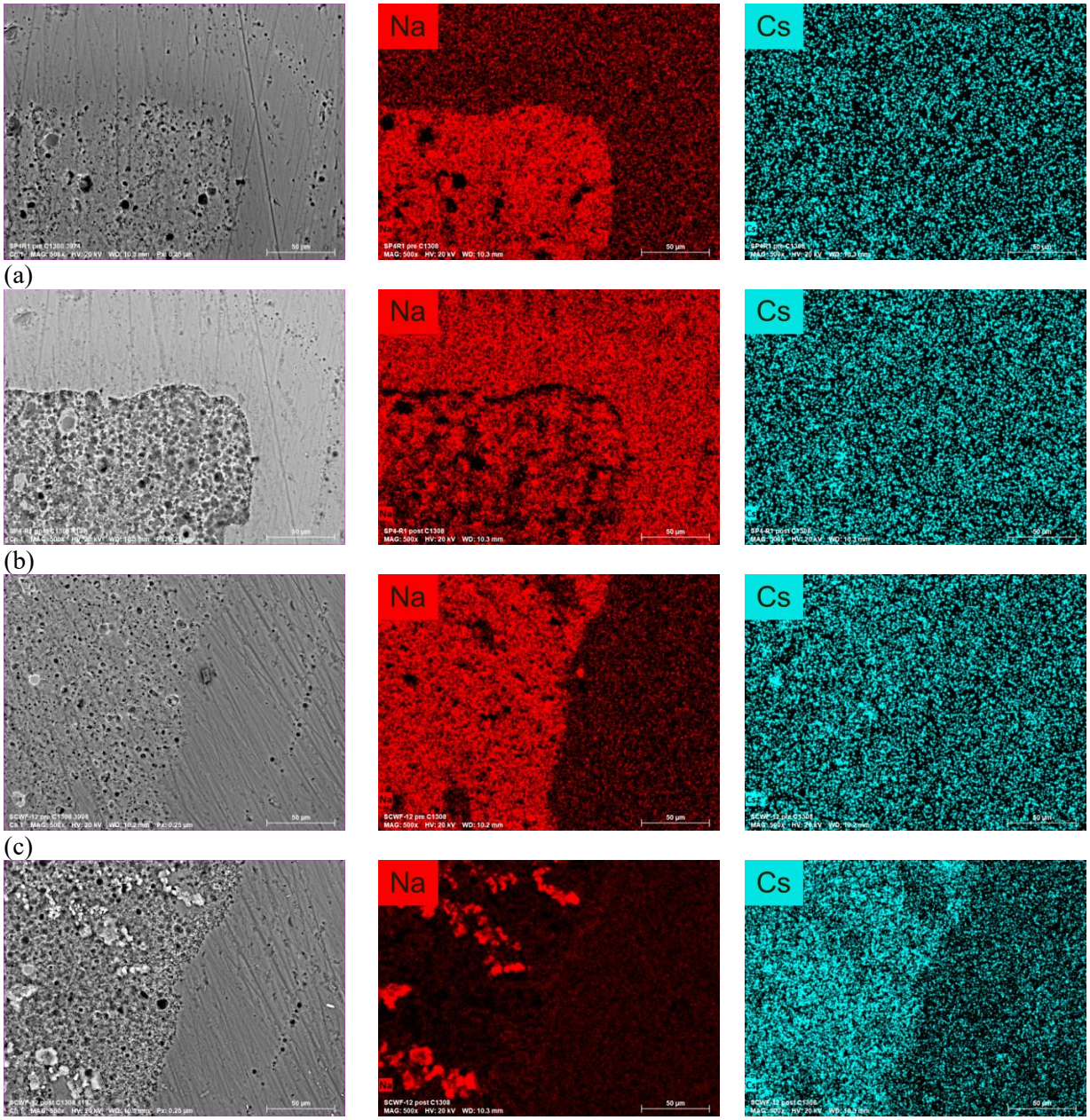

Figure 16: BSE images and corresponding EDS maps for Na and Cs, for SCWF-4 (a) before and (b) after ASTM C1308 testing, and for SCWF-12 (c) before and (d) after ASTM C1308 testing.

4. SUMMARY AND RECOMMENDATIONS

CWF materials were successfully produced using ORX salt representing waste salt from an all-LiCl flowsheet. The products were visually similar to materials made previously with ERX salt representing processing waste from electroreduction and drawdown with LiCl-KCl eutectic salt in terms of encapsulation and porosity, complete conversion of Zeolite 4A to sodalite and formation of by-product halite encapsulated in the glass and sodalite domains. The fabrication of simplified ceramic waste form products with ORX salt at various salt loadings (5, 7.5, 10 wt%) and with ERX salt (7.5% waste loading) revealed several insights into the materials chemistry. The absence of NaCl in the ORX salt did not inhibit the formation of sodalite, even at the highest salt loading of 10 wt%. As generation of sodalite in the waste form depends entirely on the exchange of Na in the glass for Li in the salt, this indicates the soda content of NBS4 glass is sufficient to accommodate a variety of waste salt chemistries in CWF materials without constrained sodalite generation at the glass/Zeolite 4A mass ratio used. Microstructures of products indicated that they consolidated well with similar levels of open porosity to CWF materials made previously with the baseline process. The porosity was not attributed to halite inclusions in the glass binder or sodalite domains.

The microstructure of the generated sodalite domains was found to be similar to that observed in previous SCWF materials made with surrogate LiCl/KCl waste salt and was fully encapsulated in the binder glass. For materials made with 5 wt% ORX salt, a relatively low fraction of sodalite domains were found to contain a Cs-enriched phase which is likely Cs-pollucite. This phase was not observed in materials with higher salt loadings, which suggests that the driving force for this may be localized depletion of Cl due to sodalite generation, which drives Cs into oxide phases. At all salt loadings, sodalite domains were also found with halite inclusions, indicating that the salt is readily transported to and occluded within zeolite domains during direct processing.

In all cases, salt inclusions were found to consist predominantly of NaCl, and were contained exclusively as inclusions either in the binder glass or within sodalite domains in SCWF materials made with 5 and 7.5 wt% ORX salt. However, excess halite was found at the top surface of SCWF-12 made with the highest salt loading of 10 wt% , likely due to gravity driven separation of the lower density molten salt. Halite was observed either as inclusions in the binder glass or at the surface of the waste form was found to contain excess Cs (co-located with excess Sr), which is likely the consequence of the elevated Cs and Sr contents in the LiCl based waste salt. This suggests that there is a limit to the quantity of Cs which can be incorporated into the CWF before it enters the salt phase, and an upper limit total salt capacity. Complete encapsulation of halite phases within the binder glass is limited to a LiCl salt loading <10 wt% based on ORX salt. The capacity limit for ERX salt remains to be determined.

ASTM C1308 durability testing of ceramic waste forms found that the initial release of salt constituents (Li, Na, Cl) was correlated directly with waste form salt loading. Due to the elevated content of fission products surrogates in the ORX salt chemistry, this also resulted in increased initial release of Cs which had not been incorporated into the binder glass during processing. For the waste forms made with 5 and 7.5 wt% salt loadings, most Cs was within halite inclusions that were encapsulated in the binder glass. In comparison to SCWF materials made with LiCl-KCl based ERX salt, both the initial release and release rate of Cs were higher in materials made with LiCl-based salt, due to the higher Cs content of the salt. The release rate based on B was lower in products made with LiCl based salt at all loadings, compared to that made with LiCl-KCl based salt, suggesting that the durability of the binder glass was improved by ion exchange of Na and Li (and absence of K).

Release rates based on Si were significantly higher for LiCl salt-based materials made with 7.5 and 10 wt% salt, compared to LiCl-KCl based materials made with 7.5 wt% salt. Considering that the release rates for B were lower overall, this suggests that the exclusion of NaCl and KCl from the salt chemistry results in a

decrease in the durability of sodalite domains over the timespan tested. However, at 10 wt% salt loading, post-C1308 test imaging by SEM-EDS indicated an enrichment in Cs occurred within sodalite domains, suggesting that the Cs-enriched phase within the domain degrades at a lower rate than sodalite.

The above effects are strongly related to the change in salt chemistry. Analysis of ASTM C1308 test solutions taken at the first day indicate the concentration of Li in residual halite was very low (<1 wt% in all cases). This indicates that at all salt loadings tested the conversion of LiCl to NaCl by ion exchange with the glass is effectively complete. This is likely the consequence of the higher affinity of Li for the glass phase compared to Na, K, or Cs, which may drive these cations out of the glass phase and into lower durability phases.

These results overall indicate that CWF products can be made successfully with LiCl based salts by using direct processing owing to the high-soda content of the NBS4 glass. The waste forms would be uniform with low open porosity, and with full conversion of zeolite to sodalite. An upper limit to the salt loading capacity exists between 7.5 and 10 wt% before excess halite will begin to separate. Elevated fission product loadings will encourage active metal fission products to remain in the halite phase, however these halite inclusions are encapsulated within the binder glass at suitably low salt loadings. The durability of the binder glass phase is higher in CWF made with LiCl based salts, however the durability of sodalite domains is decreased slightly. Lowering the salt loading to 5 wt% effectively improves the CWF durability and retention of Cs, but at the cost of total waste form volume.

REFERENCES

ASTM (2025a). *Standard Test Method for Accelerated Leach Test for Measuring Contaminant Releases from Solidified Waste*. C1308-21. ASTM-International Annual Book of Standards volume 12.01.

ASTM (2025b). *Standard Test Methods for Determining Chemical Durability of Nuclear, Hazardous, and Mixed Waste Glasses and Multiphase Glass Ceramics: The Product Consistency Test (PCT)*. C1285-21. ASTM-International Annual Book of Standards volume 12.01.

C. W. Bale, et al. (2016), *FactSage Thermochemical Software and Databases, 2010-2016*, *Calphad, vol. 54, pp 35-53,* <www.factsage.com>

Ebert, W.L. (2005). *Testing to Evaluate the Suitability of Waste Forms Developed for Electrometallurgically Treated Spent Sodium-Bonded Nuclear Fuel for Disposal in the Yucca Mountain Repository*, Argonne National Laboratory report ANL 05/43.

Ebert, W.L., Frank, S.M., and Riley, B.J. (2016). *Designing Advanced Ceramic Waste Forms for Electrochemical Processing Salt Waste*. DOE NE report FCRD-MRWFD-2016-000038. Argonne National Laboratory.

Ebert, W.L., Riley, B.J., and Frank, S.M. (2017). *Test Plan for Salt Treatment and Waste Form Development*. DOE NE report NTRD-MRWFD-2017-000191. Argonne National Laboratory.

Ebert, W.L. (2024). *Simplifying Ceramic Waste Form Processing*. Argonne report ANL/CFCT-24/7. Argonne National Laboratory.

Gesualdi, J.E. (2025). *Small-Scale Assessment of Simplified Ceramic Waste Form Processing*, Argonne National Laboratory report ANL/CFCT-25/15.

Priebe & Bateman (2008) "*The Ceramic Waste Form Process at Idaho National Laboratory." Nuclear Technology, 162:2 pp 199-207.*

Lambregts, M. J. and S. M. Frank (2003). *"Characterization of cesium containing glass-bonded ceramic waste forms." Microporous and Mesoporous Materials 64(1-3): 1-9*.